8-2012

The Influence of Coating Structure on Sheet-Fed Offset Ink Setting Rates

Ting Chen
Western Michigan University

THE INFLUENCE OF COATING STRUCTURE ON SHEET-FED OFFSET INK SETTING RATES

by

Ting Chen

A Thesis
Submitted to the
Faculty of The Graduate College
in partial fulfillment of the
requirements for the
Degree of Master of Science
Department of Paper Engineering, Chemical Engineering and Imaging
Advisor: Margaret Joyce, Ph.D.

Western Michigan University
Kalamazoo, Michigan
August 2012

THE GRADUATE COLLEGE
WESTERN MICHIGAN UNIVERSITY
KALAMAZOO, MICHIGAN

Date 06/04/2012

WE HEREBY APPROVE THE THESIS SUBMITTED BY

Ting Chen

ENTITLED The Influence of Coating Structure on the Sheet-fed Offset Ink Setting Rates

AS PARTIAL FULFILLMENT OF THE REQUIREMENTS FOR THE

DEGREE OF Master of Science

Paper Engineering, Chemical Engineering, and Imaging
(Department)

Margaret Joyce
Thesis Committee Chair

Paper and Imaging Science and Engineering
(Program)

Dave Smith
Thesis Committee Member

Paul D. Fleming
Thesis Committee Member

APPROVED

Susan A. Stapleton
Dean of The Graduate College

Date August 2012

THE INFLUENCE OF COATING STRUCTURE ON SHEET-FED OFFSET INK SETTING RATES

Ting Chen, M.S.

Western Michigan University, 2012

Much attention has been paid to the study of quickset ink setting as a complex ink-coating interaction. Offset ink setting rates are typically measured as ink splitting forces versus time and the slope of the regression line obtained from a plot of these measured values is reported, but scant attention has been paid to the deviations from that straight line. An initial slow ink setting rate is desired to minimize back-trap mottle, carryover picking and piling and enhance ink gloss; then a faster ink setting rate during sheet delivery to the pile is desired to reduce the likelihood of ink set-off, marking and scuffing and to increase product turn around efficiency.

In this work, the relationship between coating structure and the slope of the rising ink setting curve was examined. Coatings of different binder levels, binder polarity and carbonates with different particle sizes were applied to a commercial wood containing paper, using a cylindrical laboratory coater. The coating structures of the coated samples were characterized using mercury porosimetry and surface energy measurements. The Deltack force-time curves were then mapped out for each coating in time intervals small enough to detect inflections within 3s. This novel interpretation of ink setting provides fresh insights into the ink setting process.

ACKNOWLEDGMENTS

I would like to express my sincere gratitude to my thesis committee members, Dr. Margaret K. Joyce, Dr. Paul D. Fleming and Mr. Dave Smith, for their kindly advice, guidance, and assistance throughout my thesis research and beyond that.

My gratitude is extended to the industrial sponsors from Paper Technology Foundation (PTF) in Western Michigan University for their financial support for my study and research. Thanks Mr. Matt Stoops for teaching and assisting me with my experiments. I also appreciate Brian Ninness, Greg Welsch, Nick Nicholas, Mark Pollock and Tom Boyle from Styron for providing both the latex samples and first set of Deltack measurements.

Finally, my deepest gratitude goes to my parents, for their love, support, and encouragement for my life and study.

Ting Chen

TABLE OF CONTENTS

Table of Contents—continued

CHAPTER

LIST OF TABLES

LIST OF FIGURES

List of Figures—continued

CHAPTER I

INTRODUCTION

Offset printing is one of the major printing processes used to print coated papers and paperboards. Its application of a high tack oil-based paste ink and fountain solution make the ink setting rate on press critical to the runnability on press, especially on the coated papers. The ink setting rate, typically measured as ink splitting forces versus time, has a great effect on the runnability and printability of the offset press.

An ink that sets too fast at the beginning can aggravate back-trap mottle, carryover picking, piling and reduce ink gloss, while an ink that sets too slowly will increase the likelihood of ink set-off during sheet delivery to the pile, increase the occurrence of marking and scuffing and reduce product turn around efficiency. To optimize the sheet-fed offset press, it is thereby desired to ensure a slow-to-fast ink setting rate change on this press.

Although much has been done in the pressroom by the press and ink manufacturers to optimize the ink setting rates, the idea of re-engineering the paper coating or the quickset ink to provide a dramatic acceleration in ink setting rate just before sheet delivery has not been explored. However, a screening of commercial inks and experimental coating formulations on a Deltack printability tester indicated that some inks exhibit either a delay or a drop in tack before they rise (as tested on conventional fast setting coated stock) [1]. For some of the coated papers studied, a slight concave curvature was observed in the ink splitting force vs. time profile, even though they were not intentionally designed to impart such a curved ink setting profile

[1]. These observations indicate that either an ink or a paper could be designed (or the properties of both coordinated) to provide an ideal ink setting behavior.

In order to control the ink setting rate, the ink and coating interactions must be better understood. To-date, the variations in ink setting rates have been observed from point-to-point on a millimeter scale across a coating surface and correlated to back-trap mottle [2], but the variations with respect to inflections or turning points in the force-time profile have been limited strictly to the maximum force plotted on the ordinate axis: where tack rise gives way to tack decay. So, the literature contains little discussion of deviations from the ideal straight line in the tack rise portion of the curve, which is largely because instrumentation with sufficient repeatability and temporal resolution only recently has become available. Therefore, the objectives of this study were:

- To demonstrate the ability of a newly-developed prüfbau Deltack printability tester to detect smaller but repeatable tack changes than could be previously detected.
- To discuss the impact of coating structure on the setting rate of a quickset offset ink.
- To identify coating formulations capable of providing a desired slow-to-quick ink setting rate profile (an example is shown in Figure 1).

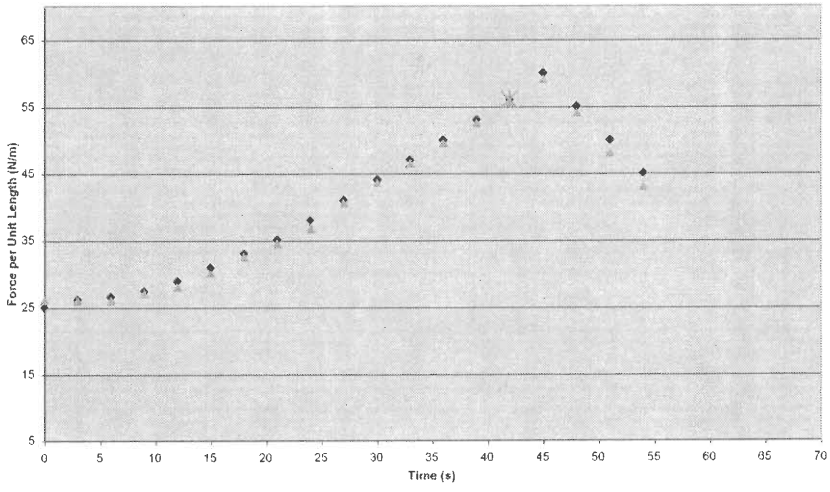

Figure 1: Example of a desirable ink setting force-time profile [3]

CHAPTER II

REFERENCES REVIEW

2.1 Overview of Offset Printing

Offset printing, short for offset Lithography, is one of the major printing processes used to print coated paper and paperboard. The major units of operation involved in this process are digital image preparation, plate preparation, printing, and finishing [4]. The principal difference between the offset printing process from the other printing processes is its use of a blanket in the image transfer process. Lithography is an indirect printing process, which means that the image is not directly transferred from the image carrier to the substrate. Instead, it is transferred to a blanket, which carries the image to the substrate.

The basis of technology for the offset printing process is that oil and water to do not mix. On the basis of this understanding, a plate is created to have hydrophobic/oleophilic areas (image areas) and hydrophilic/oleophobic areas (non-image areas). As shown in Figure 2, after pre-wetting the plate with an aqueous fountain solution (water plus additives), the hydrophilic, non-image areas of the plate are wetted. After being wetted, the printing plate then comes into contact with the oil-based offset ink. The ink wets the hydrophobic areas of the plate (image area) to form the image. The image is then transferred from the plate cylinder to a rubber blanket cylinder, hence the term offset. At last, the image is transferred to the substrate (typically paper or paperboard) backed by an impression cylinder [5].

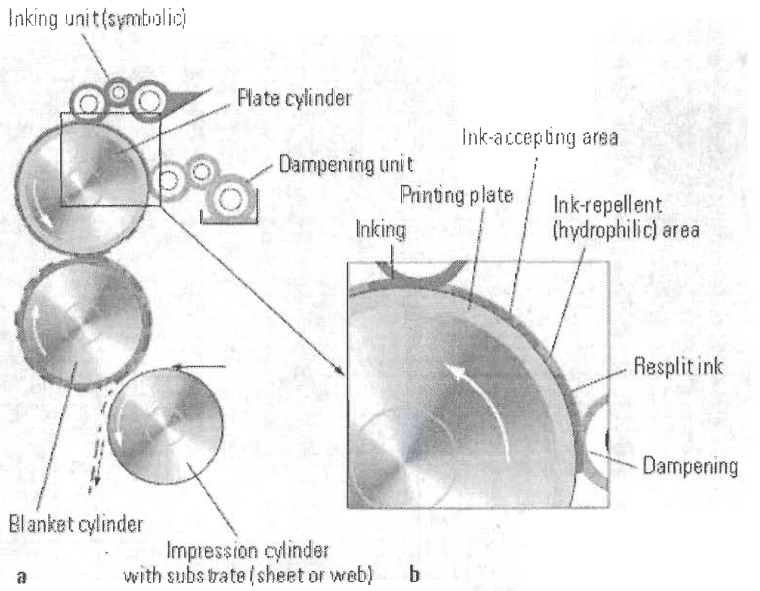

Figure 2: Offset printing unit [6]

To achieve good wetting of the non-image (hydrophilic) areas of the plate by the fountain solution, the surface tension of the fountain solution should be reduced by means of additives, such as Gum Arabic and Isopropyl Alcohol (IPA). However, care must be taken not to reduce the surface tension of the fountain solution too much for this will cause the over-emulsification of the ink and fountain solution, resulting in an unclear separation of the image and non-image areas on the plate [6].

According to different transfer mechanisms, offset presses can be classified into sheet-fed and web-fed. A sheet-fed offset press prints on individual sheets of substrate (paper, foil, film and thin metal) at a lower machine speed than a web-fed press, which prints on a continuous roll of substrate (mostly paper) [7]. The sheet-fed offset press can process substrates of different sheet sizes and basis weights. Moreover, waste sheets can be used for make-ready (to set up the press, for plates & inks) to reduce the costs of production. However, wasted sheets do bring some

disadvantages to the sheet-fed process; they are often dusty and offset dust particles can transfer onto the blankets and plate cylinders resulting in "hickeys" on the printed sheets [8]. The color combinations on a sheet-fed offset press can range from one to four-color prints up to twelve-color prints (with perfecting). In-line or off-line finishing operations, such as coating, imprinting, numbering, perforating, and punching are popular technologies that can be performed in-line with the press [6]. The addition of these flexible production options makes the lithographic printing process relatively economical for a wide range of print volumes. It is commonly used for the printing of short-run magazines, brochures, letter headings, and general commercial (jobbing) printing etc.

2.2 Ink Formulation and Offset Inks

Printing inks are made of various mixtures of chemicals that are principally determined by the printing process, transfer mechanism (sheet-fed or web-fed), and drying to be used. The ingredients of an ink are shown in Figure 3. Colorants (pigments, dyes), vehicles (resins or binders), additives and carrier substances (diluents, solvent) are some of the many different chemicals that can be used [6]. It should be noted that the concepts of varnish and vehicle are often interchangeable. Varnishes are considered as binders, while vehicles consist of varnishes, carrier substances and/or additives, i.e. all of the ink except the colorant [9, 10].

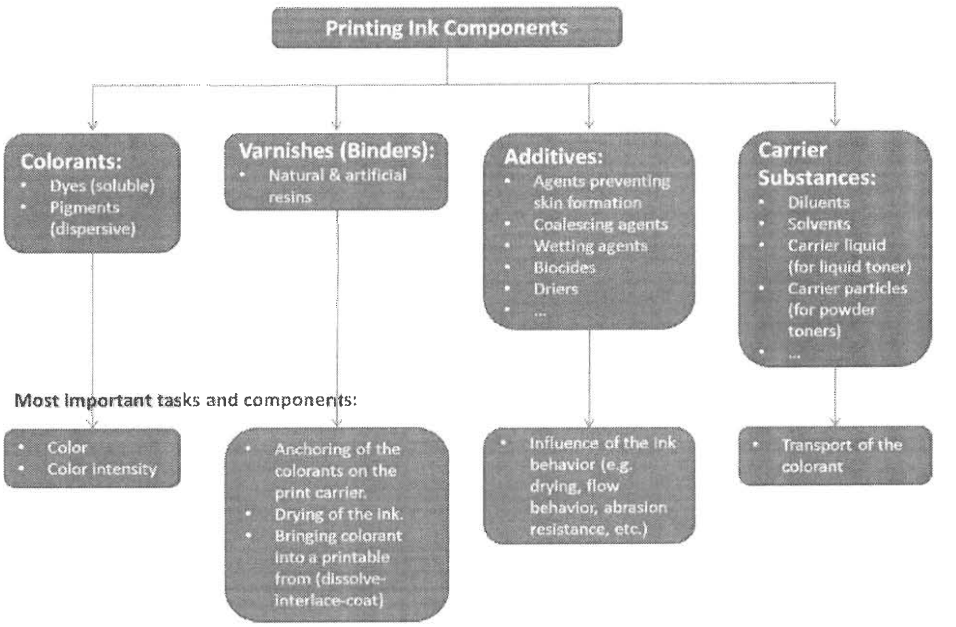

Figure 3: Ink components and their functions (modified from Kipphan [6])

Colorants give color to the ink. They are divided into pigments and dyes. Pigments (usually 5%-30% by weight) are more commonly used than dyes, due to their advantages of better light-fastness and lower price. Pigments in the inks exist as solid particles and/or molecular agglomerates for which a binder is required to adhere them to the substrate. The pigments on the surface, with a few pigments lying just beneath the surface, absorb and disperse the light to create the perceived color [6]. In contrast, dyes exist as molecules, so they have higher efficiency of selective absorption and provide a wider color gamut than pigments. The dye molecules can be dissolved in the base liquid and most dyes can bind directly to the substrate surface. Pigments are organically or inorganically colored, white or black. Organic pigments are used for process inks because of their good transparency, while inorganic pigments have better opacity. Dyes can be converted to PMTA (Phosphoric, Molybdic, Tungstic Acid, etc.) pigments [6] through their reaction with

Phosphomolybdic Acid and Phosphotungstic Acid. The important properties of a pigment in an ink are tinctorial strength, opacity, gloss, shade, durability, particle size, specific gravity, refractive index, hardness or texture, wettability, dispersibility, lightfastness and chemical resistance [9].

A vehicle is comprised of binders/resins (usually 20%-40% by weight), carrier substances (usually 30%-50% by weight), and/or drying oil [9, 10]. The pigments are finely dispersed in the binders, which protect them from agglomeration. During drying, the binders dry on the substrate, adhering the pigment particles to the substrate surface. The carrier substances, such as diluents and solvent, affect the ink setting rate and ink drying mechanism.

Additives (typically 0-10% by weight) are the compounds used to improve the ink characteristics, such as ink tack, drying, flow behavior and rub resistance. The common additives are reducers (to reduce the tack and stickiness of the ink), driers (to speed oxidation and drying of the oil vehicle), waxes (to improve rub resistance and slip properties), anti-skinning agents / antioxidants (to prevent premature drying and skin formation on the surface in the can or in the ink fountain) [8]. Besides these functions, the compatibility of additives with the ink vehicles should be taken into account during the formulation of the ink.

Offset inks are typically paste inks (dynamic viscosity is 40000-100000 cP). An important aspect of the formation of the non-image area is the contrast between the low viscosity of the fountain solution and the much higher viscosity of the ink. If the ink were too low in viscosity, the water might be less inclined to undergo the sacrificial split. For a thin ink, it would be difficult to obtain the lateral control of the ink film thickness across the rollers, the ink would drip down away the rollers (by gravity), centrifugal forces would fling the ink into the air and the fountain solution

would be over-emulsified in the ink. A higher viscosity of the transferred ink film narrows the viscosity gap between the fluid ink and the final solid phase so that the ink solidification takes less time. If the ink viscosity were too high, it would require additional energy to distribute the ink, generating additional heat and increasing the cooling costs. An ink that is too thick would not be able to emulsify sufficient fountain solution to carry it away from the plate. Extreme tackiness would be too destructive to typical paper substrates and it would not be able to recover from ink splitting sufficiently to level in time to give a smooth printed film.

It is also important that the ink can store a certain portion of the fountain solution, which is taken-up via contact with the plate or directly via the damping unit [1]. The offset inks should also be thixotropic, so they can flow readily through the ink roller train and penetrate into the substrate after ink transfer from the blanket to produce a thin uniform ink film (0.5-1.5 microns) [11].

In the formulation of offset inks, pigments (10%-30% by weight), which consist of solid, irregularly-shaped particles of 0.1-2 microns size, can be either organic or inorganic. A vehicle essentially contains hard resins (20%-50% by weight) with a high proportion of colophon, alkyd resins (0-20% by weight), and portions of vegetable oil (0-30% by weight) or mineral oil (20%-40% by weight) and various drying agents (<2% by weight) [6]. Furthermore, various additives, such as driers, waxes and anti-skinning agents etc., are added in small amounts to improve the flow properties, drying and print quality of offset inks.

2.3 Paper Coatings

It is well known that the properties of a paper have great influence on print quality. The application of a coating can improve the optical, print and functional

properties of paper, such as gloss, brightness, smoothness, ink density, dot roundness, oil resistance and water resistance, respectively. Though about 80% of all coated paper properties depend on the properties of the base paper [12], a coating is still required to fill the voids in the paper in order to create a uniform surface for best print quality.

A coating is comprised of a coating pigment, binder and additives. The weight fraction of each component in the dry coating varies according to the coated grade of paper being produced, but commonly 80%-95% of the coating is pigment, 5%-20% of the coating is binder and 2% of the coating is additives [11]. Water is also an essential component of the formulation. It makes it possible to mix all the components together, to transport the coating and to apply the coating evenly on the base paper. The content of water can be up to 30 wt. %. After drying, the coating layer may contain up to 50% pigment, 20%-30% binder, 25%-35% air and 1%-3% additives (% by volume) [13].

The different units of operation involved in the coating and finishing of paper and board and a list of the important coating properties to each process are provided in Table 1.

Table 1

Critical properties of coatings required in different processes

Processes	Critical properties of coatings
Coating	Rheology Water Retention
Drying	Film Formation Porosity
Finishing	Calenderability Structure Stability
Printing	Porosity Surface Energy Pick Strength Paper Gloss Printability

A general sequence for the order of addition of coating components is shown in Figure 4. The sequence of addition is important to prevent or minimize the interaction between coating components, which may lower the efficiency of their properties [12].

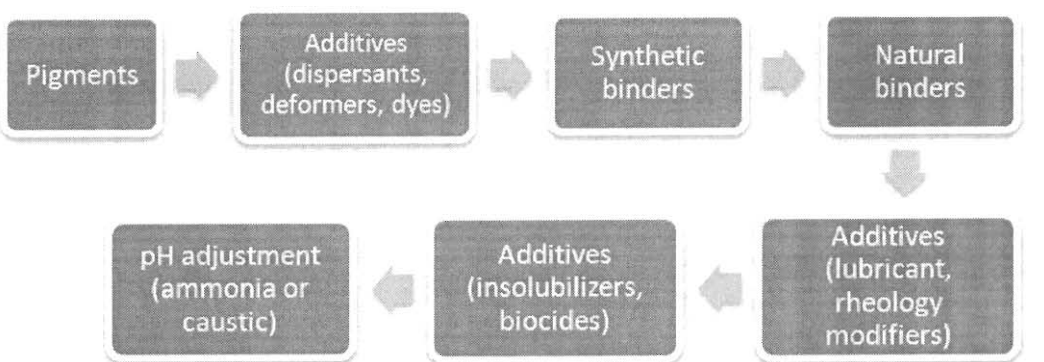

Figure 4: General sequence of addition during coating makedown

2.3.1 Coating Pigments

The pigments used in a coating can be divided into main pigments and specialty pigments [12]. Clay/Kaolin, Ground Calcium Carbonate (GCC) and Talc are the main pigments, while Precipitated Calcium Carbonate (PCC), Calcined Clay, Plastic Pigments, Alumina Trihydrate and Titanium Dioxide are the specialty pigments used. Specialty pigments are used to compensate for the lack of properties obtainable by the main pigments alone. They comprise a small fraction of the total pigment used in a coating formulation and as a rule of thumb, consist of no more than 10% of the total pigment used in a formulation [12].

2.3.2 Coating Binders

Similar to the resins used in inks, a binder in a coating formulation binds the pigment particles with each other and to the base paper, while filling part of the voids between the pigment particles [12]. It has a great impact on the runnability of the coatings on the coaters (rheological properties, water retention, drying etc.), the final properties of the coated paper (stiffness, strength and optical properties etc.), and the printability of the coated paper (ink-coating interactions) [12].

There are two types of binders: natural binders (starch and protein) and synthetic binders (styrene butadiene and styrene acrylic latexes, PVAc and PVOH) [14]. The selection of binder should take into account the end-use requirements of the coated paper, the rheological properties of the coating, the drying capability on machine, and the other components present in the coating, especially the pigment type of the coatings to assure the desired coating strength, optical properties and print properties are achieved.

2.3.3 Coating Additives

Coating additives are used at small dosage levels but are very important to the end-use performance and runnability of the coating on the coater. The most common types of additives are dispersants, lubricants, pH control agents, defoamers, water retention aids, rheology modifiers, optical brightness agents (OBA), dyes and colorants, insolubilizers, biocides/preservatives, and other functional agents (anti-skin agents, special surfactants etc.) [12].

2.4 Ink Setting and Drying

The drying of the ink refers to all processes after ink transfer onto the substrate. It is actually a multiple of processes which includes physical effects (penetration and evaporation) and chemical effects (oxidation and polymerization) (Fig. 5). Specifically, the ink changes before being dried by the driers are all termed as "ink setting". Ink setting mainly occurs before the oven evaporation of the drying oils or polymerization of the ink binders, through the reaction with oxygen [6].

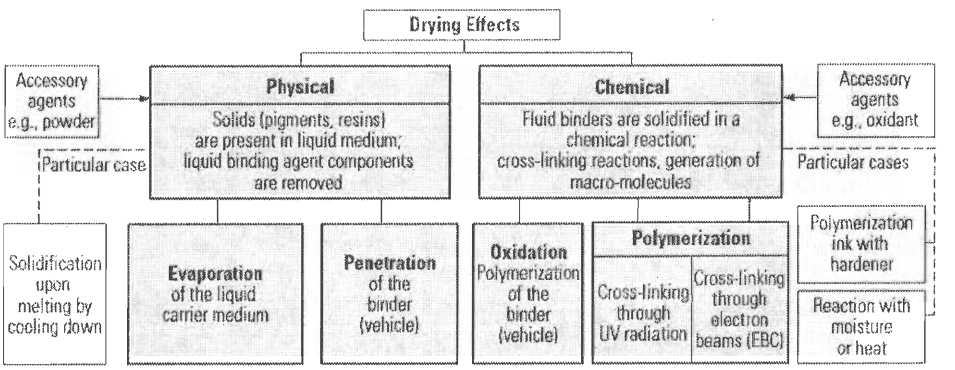

Figure 5: Overview of ink drying effects [6]

Without the following processes in the offset printing process, ink leveling

and setting alone may take place in less than 15 min, while the drying of the ink needs several hours [15]. An appropriate ink setting and drying rate is desirable to provide a prerequisite for the reliable printing, finishing, and quality of the printed products.

The process of ink setting is so crucial to the runnability and printability of the offset press that the contribution of coating structure and ink properties to the ink setting rates has been the object of focus over the past thirty years [16-19]. Previous research reveals that there are four major ink-coating interactions happening during the ink setting process (Fig. 6): 1) the formation of ink filaments that break immediately after ink transfer 2) the release of ink fluid phase components into coating pores and the separation of ink constituents 3) the capillary absorption resulting from the porous coating structure and 4) the diffusion of ink diluents into the polymer components of the coating layer. From another perspective, the complex ink-coating interactions can be ascribed to the physical structure of coated paper and the chemical properties of ink and coating components.

The formation of ink filaments is essential for obtaining good print gloss, which will be talked about in section 2.5.1.

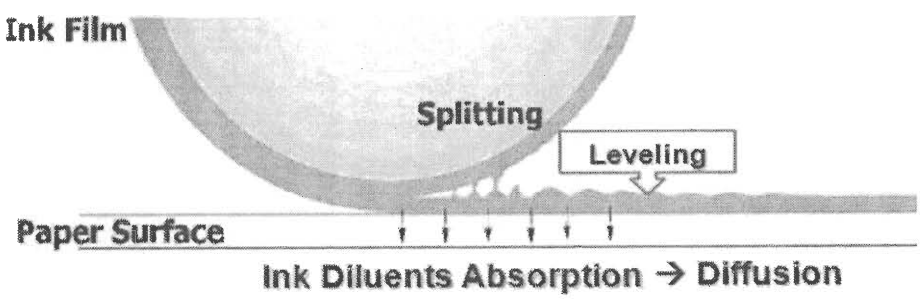

Figure 6: A tentative illustration of the ink-to-paper transferring process

Several researchers have reported that the release of ink fluid phase and the

separation of ink constituents are generated by the numerous capillaries in the porous coating structure right after ink splitting [17, 18, 21]. Ström, Gustafsson and Sjölin [19] verified that the offset ink setting process is initiated by the separation and removal of oil from the ink film through the absorption of these components into the paper coating and that none of the pigment particles and binders or only small amounts of them go with the ink oil into the coating while the oil is being absorbed (Fig. 7).

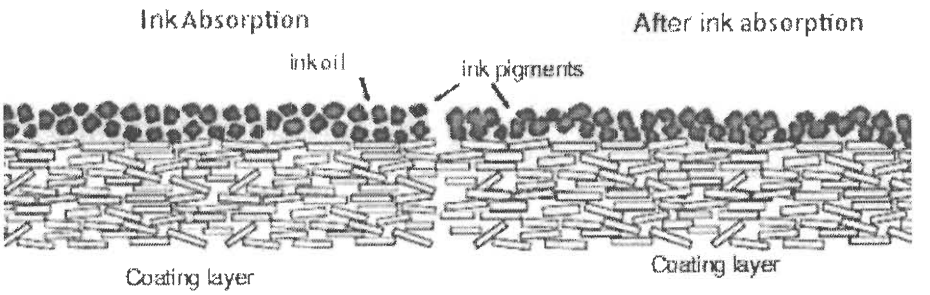

Figure 7: Differential ink absorption on coated paper [20]

Diluent release is controlled by the low solubility of the ink resins in the diluent oil. There is a wide variation in the kinetics of this phase separation. Conventional quickset inks start to build tack and viscosity between zero and about four seconds after printing and continue for about 50 s before the measured ink tack retreats. Rousu *et al.* [13, 21] clarified this differential absorption of the ink components from different ink formulations on a series of well-defined coating layers of various chemical and physical characteristics. It was proposed that there was adsorptive chromatographic separation of the ink constituents at the beginning of the ink absorption process, which was induced by the remaining ink pigments and resins on the coating surface and that the chemical components of an ink are separated on

contact with the paper coating due to their different adsorption characteristics, which arise from the coating chemistry, surface area, and morphology variables.

The porosity of a coating structure is a dominant factor in controlling ink setting rates. The influences of pore size (diameter), pore volume and pore number/pore density have been discussed intensively. Xiang and Bousfield [22-24], Kishida [25] and Donigian *et al.* [26] agreed that either an increase in the total pore volume with a fixed average pore size (diameter) or reduction in pore size (diameter) with a fixed pore volume can yield a higher ink setting rate. However, the number of pores and their size (diameter) together affect the measured pore volume so a new term was brought in by Preston *et al.* [27] who defined the number of pores per unit area as "pore density". As such, a higher pore density sets ink faster at a fixed pore size (diameter). Therefore, it is necessary to develop an understanding of the relative importance of each factors talked above. A model to predict the ink setting rate of coated paper was generated after analyzing the ink setting rates of a multitude of coated papers [5]:

$$V = N R^{3/2} k t^{1/2}$$

Where,

V=the volume of distillate removed from the ink into the coated paper;

N=the number of pores/ unit area;

R=pore radius;

k=constant;

t=the time to the maximum tack force

Regardless of this finding, a comparison of the data calculated from this model with the data from measurements made, showed that a gap existing between the two requires further consideration of this concept.

The properties of the pores in coated papers are controlled largely by the pore size distribution (PSD) of the coating pigments. As a rule of thumb, coarser pigments produce larger pores but of lower pore density (fewer pores), while finer pigments (typically those with a large proportion of the size distribution finer than 0.25μm) result in a greater pore density and a faster ink setting rate. In addition to this understanding, steeper/narrower pore size distributions tend to give larger pore sizes for a given number of pores, which speeds up the rate of ink setting [5, 24-26].

To understand the mechanism of ink setting, it is important to investigate the mechanism of fluid transport into porous structures. Gane *et al.* [28-30] carried out a series of experiments to better understand the connection between the two. In their work, [28-29] a series of liquids of different polarities and viscosities were brought into contact with a wide range of porous coating structures and by use of image analysis techniques, the relevant phenomena of spreading, penetration and adsorption of the ink into the different coating structures were studied. These observations supported the belief that three transitional conditions of fluid transport exits during the ink setting process and showed that in order to obtain sharply defined printed dots with the ink pigment particles lying close to the surface, a balance of optimal ink spread/penetration ratio and fast setting within the runnable limits of the press is required. Meanwhile, a uniform distribution of the absorption controlling parameters on the surface is required to prevent low print density and gloss mottle. It was also indicated that the detected void volume decreases as a function of decreasing oil polarity. At longer time intervals, a transition from the filling of pores to the draining of the pores occurs, when the liquid remains as an adsorbed layer on the capillary walls after being differentially drawn into the finer pores and capillary networks of the coating layer. The amount of pore draining was found to be dependent on the pore-to-

throat diameter ratio and the available volume of the smaller voids. Schölkopf and Gane [30] later made a comparison of the various liquid interaction radii derived from the experimental and network modeling of porous pigmented structures. They obtained various equivalent hydraulic radii from (i) surface area/porosity correlations, (ii) imbibition, (iii) liquid permeation, and (iv) mercury intrusion at the same time compared with simulations of the structures and their interaction with liquids using Pore-Cor modeling software. The combined data indicated the existence of different pore segregation mechanisms underlying the observed phenomenological dissimilarities for the complex porous network structure.

The influences of polymeric binders have also been proven to be important to the diffusion of ink oil into the coating structure. Rousu *et al.* [31] stated that latex-oil diffusion happens when the oil molecules penetrate into the polymer latex matrix, which is triggered by the molecular movement in response to a concentration gradient. She found that an ink oil with a higher solubility parameter [(vaporization energy/molar volume) $^{0.5}$] and low viscosity in addition to latexes of a low T_g and gel% promoted the ink-latex diffusion process. It was inferred that a greater rate of diffusion could cause latex swelling to occur which sacrifices some of the available coating pores. The loss in the available coating pores results in a reduction in the ink setting rate. In addition to this finding, it was determined that an increase in the diffusion rate of ink oil and latex into a coated paper can also be attributed to an increase in the cross-linking and polarity of carboxylated styrene butadiene binders on the market (SB latex) which reduce the rate of ink setting as reported by Desjumaux *et al.* [32].

2.5 The Influences of Ink Setting Rates on Offset Printability and Runnability

The reason why the mechanism of ink setting draws much attention is due to its influences of ink setting rates on the printability and runnability of the offset press. An improper ink setting rate can result in poor print quality i.e., low print gloss, low print density and offensive print defects.

2.5.1 The Influences of Ink Setting Rates on Print Gloss

Print gloss is considered as one of the essential properties of printed paper. It basically depends on the topography and refractive index of the base paper. When comparing similar substrates, where the refractive indices are similar, the differences in gloss are caused largely by the topography. As outlined by Oittinen [33], the topography of the coated paper can be divided into macro roughness, generated by the structure of the base paper, and micro roughness, mainly determined by the size, shape, and orientation of pigment particles on the surface. Drage *et al.* [34] plotted the relation of macro/micro roughness and gloss (Fig. 8) of paper and invented a new pigment system to yield an improved balance of properties between print abrasion and brightness without affecting sheet gloss or print performance.

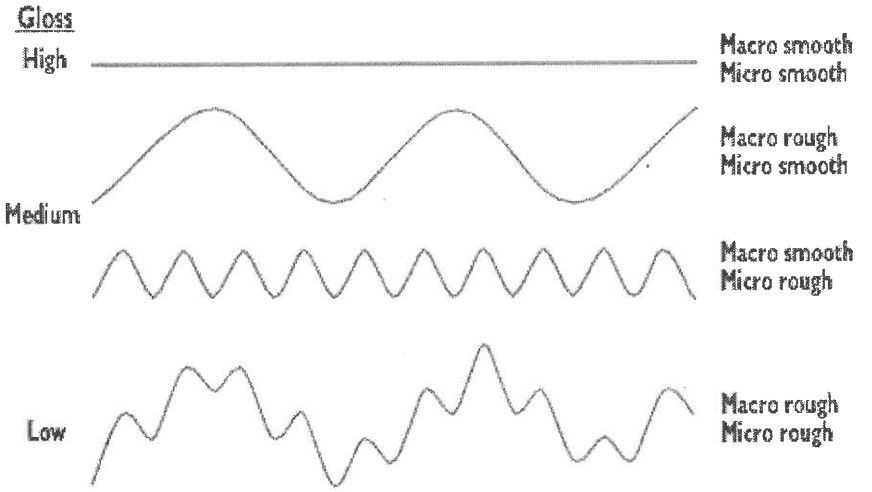

Figure 8: Macro roughness and micro roughness in combination determine gloss [34]

When talking about print gloss, the refractive index of the substrate is assumed to be the same over the initial ink-setting time intervals, though it is actually changing due to the absorption of ink oil by the coating layer. Zang and Aspler [35] revealed that the offset print gloss obtained will increase with an increase in coating gloss (or smoothness) at low ink levels, but at high ink levels, the print gloss is primarily influenced by the micro roughness or the gloss of the ink film, which in turn depends on the filament patterns produced during the ink splitting process and the absorbency of the coating layer.

The filamentation of the ink during ink splitting in the nip exit produces a very rough ink film on the surface of the paper. Thus, for good print gloss, the leveling of the ink must occur within the first few seconds of ink setting process [36-38]. Donigian [39] stated that 90% of the gloss increase in an ink film will typically occur within the first 10 s, sometimes even within the first 2 s, after the paper contacts with the blanket. This rapid procedure has been measured microscopically and the effect of

reducing the size of the filament by the decrease in ink viscosity during absorption was found by Ercan [40, 41].

On the other hand, a highly absorbent coating layer can cause low print gloss due to the reduction of the time for ink leveling. Donigian *et al.* [39] later confirmed the profound influence of coating absorbency on print gloss. In their study, fine to very fine pigments were used to significantly increase the coating-ink absorbency. The very fine coating particles produced a high pigment surface area and very fine coating pores that greatly reduced print gloss. The increased capillary pressure provided a higher driving force for the imbibition of the ink vehicle into the coating, which accounted for these phenomena. Ström and Karathanasis [15] extended the conclusion of Zang and Aspler [35] by considering the effects of coating micro roughness, ink filament patterning, ink setting rate and ink film roughness together with SEM (Scanning Electron Microscope) and AFM (Atomic Force Microscopy) image analysis. Their research confirmed that coating micro roughness strongly affects print gloss, in particular at low inking levels. A linear relation between ink film roughness and print gloss was also found. More importantly, a structure in the ink film, regarded as frozen filament patterns with feature sizes of roughly 10-100 μm, was identified for a fast setting paper but not for a slow setting paper. The presence of this structure reduced print gloss by up to 6 units.

In conclusion, a fast ink setting rate generally has a lower print gloss due to the following two mechanisms [5]:

- Ink filamentation, which produces a macro rough surface that needs enough time to level.
- A very micro-porous, fast ink setting coating does not allow sufficient time for filament leveling. It also pulls more ink oils and some resins out from the ink into

the coating layer, leaving ink pigments and extenders protruding from the surface. The protrusion of the pigments and extenders at the surface results in an increase in micro-roughness and a reduced print gloss.

2.5.2 The Influences of Offset Ink Setting Rate on Print Defects

Picking and Piling

Given the ink-coating mechanisms, ink tack (ink splitting force) increases through the absorption of the ink diluents (oils/solvents) by the coated paper as the paper back-traps down a multi-unit press. Voltaire and Fogden [42] claimed that the ink tack on the ISIT reaches a maximum in the first 100 s or even less and thereafter declines. When the splitting force approaches the point at which the coating or fiber fails, which means the ink setting is too fast, picking happens even possibly followed by piling of the coating on the blanket or plate on press. It not only produces visible damage to the print and contaminates the blanket, but it may also cause plate blinding, plate wear and "smashed" blankets. The contanminates are also manifested as carryover picking and carryover piling on downstream units. The relationship of ink setting rates to back-trap piling and micro-picking has been discussed by Donigian [43]. Therefore, the dry and wet strength of coating is of crucial importance on the printing.

Mottling

Mottle, is one of the most common print defects that occurs on the offset press. It is the irregular and undesired visual non-uniform appearance on the print image. The visual variation, spotty or cloudy appearance, could be manifested as print density, print gloss or color on the image area [44]. In terms of the different causes,

mottle can be divided into three types: back-trap mottle, wet ink trap mottle and water inference mottle [45]. Except for the last one, the other two can be ascribed to the inappropriate ink setting rate/ink tack.

Back-trap mottle is the most common form of mottle. It occurs only on a multi-unit offset press when the wet ink from the surface of the paper printed on the previous unit transfers back onto ("back-trap") the blanket of the subsequent unit. An uneven and fast ink setting rate is usually to blame for its onset and severity, though the printing speed is critical here too. It is believed that the uneven absorption of the ink diluents by the coating layer leads to a non-uniform ink setting rate, which in return causes an uneven ink split between the new ink film and subsequent blanket (Fig. 9). More seriously, it may induce coating pick and the series of problems from picking mentioned before [44].

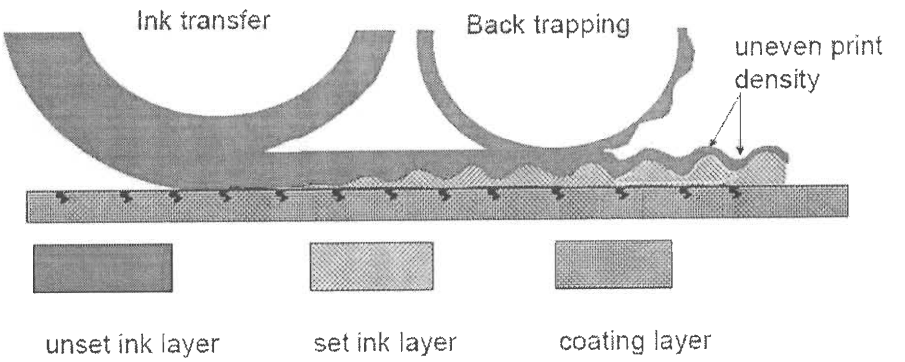

Figure 9: Process of back-trap mottling [46]

When printing with multiple colors, good ink trapping (wet ink film is printed over another one) is pursued to produce the desired print quality. The ink tack sequence thereby is paramount. If the ink tack of the previous print unit is lower than that of the next unit, the previous ink film may be pulled apart with the subsequent

ink film due to its higher ink splitting force that turns out to be bad trapping. In this case, wet ink trap mottle appears on the print image and can be more severe with more print units [46].

Ink Set-off/Blocking

When arriving at the delivery pile, the printed paper may not be completely solidified, which takes at least ten minutes to be ready for further processing and shipping. Some post press problems arise due to the slow ink setting and drying, such as ink set-off, blocking and marking along with production and shipping delays. The transference of the ink to the backside of the above sheet is considered as ink set-off. As such, the sheets in a bundle or load may stick together, blocking [44].

2.6 Methods to Optimize Ink Setting and Drying

To help the printer cope with incomplete drying of the ink, press manufacturers have created three pieces of auxiliary equipment that help to minimize the problems related to slow phase separation of so-called "quickset" inks.

- An infra-red (IR) heater warms the wet print that emerges from the last printing unit - this accelerates ink setting, however energy costs are incurred and the equipment adds several feet to the length of a sheet-fed press. Furthermore, not all inks respond positively to warmth and this behavior is difficult to measure. IR heaters are typically used together with either starch or aqueous coatings [3].
- Anti-offset starch powder is puffed onto each print as it arrives on the delivery pile. These hard microscopic particles protrude from the ink film creating an air space between the ink film and the overlying sheet. However an airborne dust is produced that contaminates the press and pressroom leading to mechanical

deterioration and high maintenance costs. Other disadvantages include a negative impact on ink gloss and increased surface abrasivity [3].

- Fast drying, clear aqueous coatings can be applied to cover the wet inks. The surface of these styrene-acrylic emulsions dries quickly to prevent set off. However, the ink is still wet underneath the film and coating application requires additional costs [3].

In addition to these processes that deal with symptoms of slow ink setting, there are two methods that promote the "ideal" instant solidification of the printed quickset ink.

- UV Curing for sheet-fed prints: exposure of the print to ultra-violet light immediately after printing. This initiates polymerization of the ink [3].
- Evaporation of the ink diluent. This has not been possible in sheet-fed printing, but this principle is widely used when printing at high speed from rolls: in a process known as heat set web offset. The long ovens require capital, energy and maintenance costs [3].

These innovations exemplify how seriously the printing industry has strived to approach the ideal ink solidification. The fact that the printer can justify the capital cost of equipment and consumables to reduce the expense of slow turnaround and spoilage emphasizes the seriousness of dealing with an ink that is still a tacky paste several minutes after application. While these innovations in ink and pressroom equipment were evolving, the paper maker was not required to modify the paper. In response to customer feedback, mills tweaked the pigmented coating to either slow down ink setting speeds, in order to minimize carryover picking and back-trap mottle and improve ink gloss, or increase ink setting speeds in order to minimize set off and blocking. Changes in ink setting speed have been limited to either raising or lowering

one slope number, not only because instruments previously lacked sufficient sensitivity but also because a good majority of quickset inks exhibit a fairly linear setting response with the majority of coated offset papers [1].

2.7 The Measurements of Ink Setting Rates

Typically, ink setting rates on coated papers are measured and reported as the slope of a straight line fitted to the rising part of the ink splitting force vs. time curve [1]. The curves are unique for each ink/paper combination and the slope, the passes to fail, and the force at failure are reported. These three components of the test result have provided data useful for predicting and diagnosing press performance, for coating development and for gleaning an insight into the complex interactions between the ink and paper coating [3].

2.7.1 The Instruments Used in Previous Research

For the last forty years, various instruments have been invented and used to measure ink setting rates. The early evolutions were the Vandercook press with a Lodcel [1] (Fig. 10) and the Ink Surface Interaction Tester (ISIT) [48] (Fig. 11).

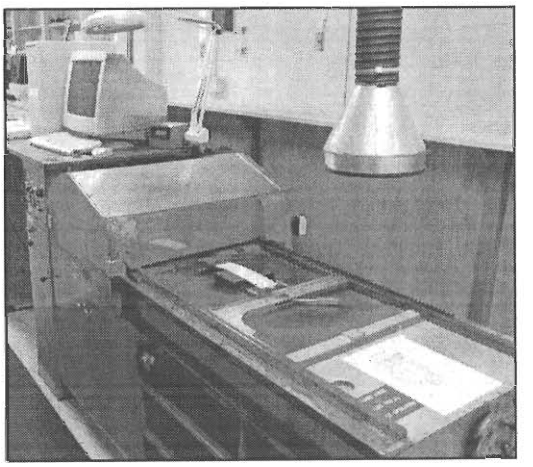

Figure 10: Vandercook press with a Lodcel [47]

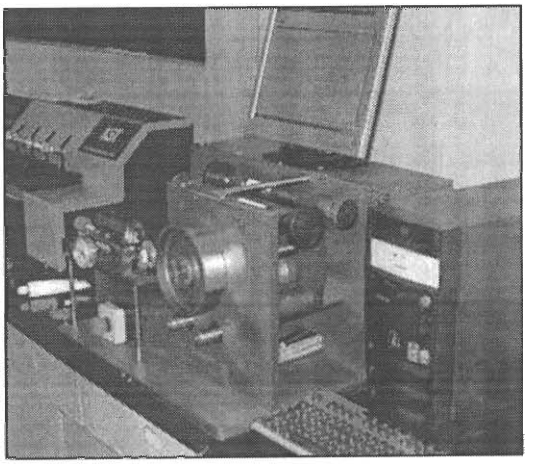

Figure 11: Ink Surface Interaction Tester (ISIT) [49]

Also known as the NPA Print and Ink Stability tester [50], the Vandercook flatbed letterpress was adapted by adding a strain gauge (Lodcel) to measure the splitting force in a moving nip. It continually back-traps the entire ink film, which enables problem diagnosis, product development, press predictions to be made and the study of ink-coating interaction mechanisms [1]. The Vandercook-Lodcel system can only run at 0.5 m/s (100 feet per minute) speed. It creates and measures a film split once every 7 s. With very fast setting ink-on-paper systems, it was found that the Vandercook-Lodcel cannot detect the rapid initial increase in ink tack. In fact, it sometimes can only detect the after-effect of a rapid rise in tack, which is typically a rapid decline [1]. The impression pressure, depending on the height of the bed, cannot be measured or controlled with this system. It requires 7-10 min for each test determination because of the necessity of a complete cleanup and redistribution of ink for every test performed [1].

At normal set speed 0.5 m/s and impression pressure 50 kgf, the Ink Surface Interaction Tester (ISIT) continually probes the fresh portions of the ink film during

splitting as shown in Figure 12 [48]. The ink must be distributed on the print disc by the IGT ink distributor under standard conditions and then is transferred approximately 1 g/m^2 onto the paper. For a quick drying offset ink, the maximum measurement time is 20 min or 4 prints. The possible time interval it can achieve is 4 to 5 s but depends on the separation between the tack disc and ink film (approximate 3 s delay in practice) [48]. However, the onset of picking is difficult to detect on this instrument and the ink setting rate is sometimes calculated as the time to reach maximum tack but force/time slopes are not usually calculated. The precision of the ISIT was quoted once as having a 20% "relative error" for tack rise time – one assumes this means the coefficient of variation (the standard deviation divided by the mean, expressed as a percentage) [27].

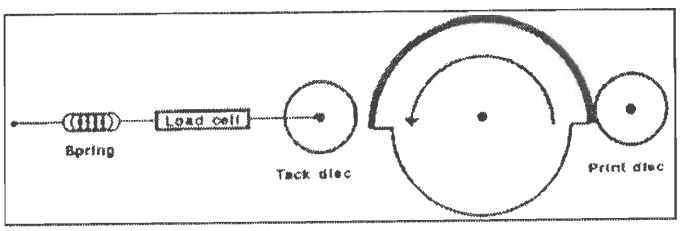

Figure 12: Schematic arrangement of ISIT [48]

Another instrument, Micro-Tackmeter [51] (Fig. 13), was invented and used by the University of Maine to measure the point-to-point changes in tack development across a paper surface of about 1 mm^2. It is not used often due to its measurement limitations, such as the undetectable amount of ink transferred to the paper, limits of contacting force (0.5 to 25 gf), inability for measurement of the coating failure force, and a large range of variation coefficients (28% to 59% for 1.1 mm diameter probe and 49% to 71% for 2.2 mm diameter probe) [51]. The shortest time interval for

measurement capture is 5 s and the motor speed is 15 mm/min [51].

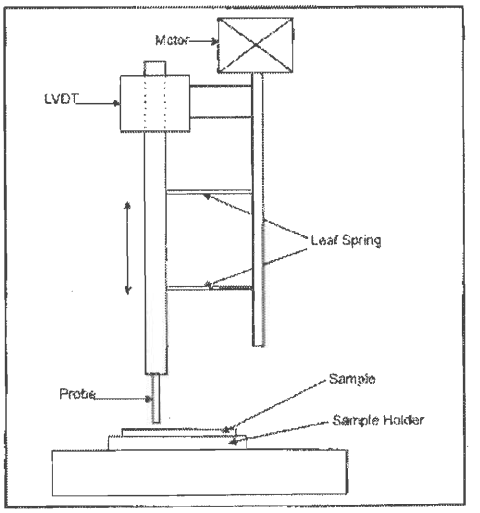

Figure 13: Schematic of Micro-Tackmeter [50]

Theoretically, an ideal instrument for the ink setting rates detection should have high level of precision, resolution, simulation, efficiency and utility. In addition, the instrument for research should also have a wide range of settings and a wide measurement scale.

2.7.2 The Newly Developed Instrument: Deltack Printability Tester

The prüfbau Deltack printability tester (Fig. 14) has the unique capability of being able to measure force-time points with both repeatable force readings over a wide range and high temporal resolution (e.g. 2 s intervals) during press-imitative, rotatory back-trapping print cycles. It has a PC-based controller and a close-to-commercial printing impression pressure and speed, the interval (cycle time) and number of intervals, and the temperature and time of ink distribution closely resembles commercial practices. This instrument was originally described by Smith *et*

al. [1, 47]. The measurement of force vs. time profiles, the force and time at which picking first occurs and calculated slope of ink tack rise by this method, provides an opportunity for the contribution of coating composition and structure to ink setting to be better understood.

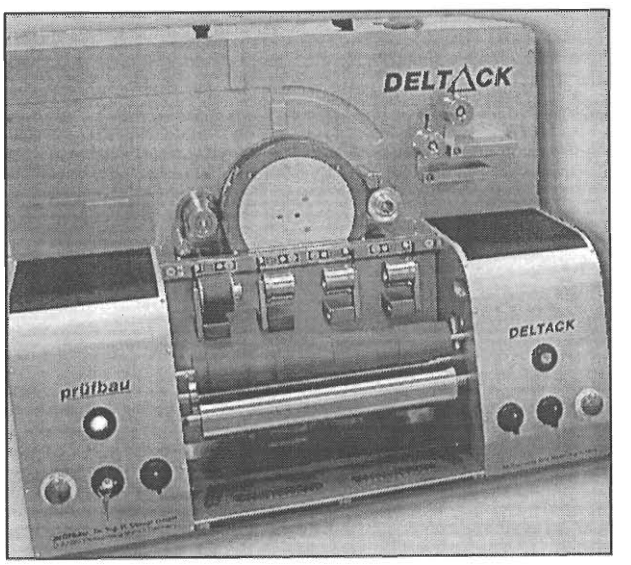

Figure 14: The prüfbau Deltack printability tester [47]

Of great relevance to the measurements in this project are the following data for each print run [1]:

- Ink splitting forces as a function of time over prescribed intervals. The measurements were performed at 3s intervals.
- The slope of a best-fit straight regression line through all "good" points. "Bad" points are objectively determined through algorithms performed in Excel that imports and calculates the data received from the instrument. The coefficient of determination (r^2) of the regression line is also calculated.
- The time of first observed pick on the print wheel is recorded. A common

preference is for "passes to fail", here we use "intervals to picking". Picking is shown on the plots as large asterisks superimposed on the force time plot. Fiber picking could also be recorded, but was not used here.

- The picking force at onset of picking. This can be considered a realistic measurement of the dry strength of the coating. Unlike accelerated single impression dry pick testing, a measured force rather than a force estimated from speed and tack (involving risky assumptions about ink's rheology) is reported. The picking force is expressed in N/m because it is measured for a 5 cm wide sample in force units of Newtons. In order to compare with other force instruments that might have different sample widths, the force readings are multiplied by 20 to derive the force that would be measured over a 1 m wide sample. Picking by this multiple impression method is seen mostly at the surface, which has the advantage of resembling surface failure seen in commercial printing. On the contrary, the instantaneous "dry pick" testing (where ink setting is not involved) typically creates failure deeper into the coating and base fibers. Furthermore, it is speculated that during multiple impression testing, the diluent has a few seconds to diffuse into the binder, plasticizing the surface polymer and reducing its capacity to resist tack forces. While during single cycle "dry pick" testing, the unperturbed surface binder could be stronger than the underlying fibers, relegating failure to any weaker elements of the entire structure.
- Automated exclusion of early force points that drop before force readings rise. Since they are repeatable, they cannot be called "noise". But they are inconvenient. These artifacts are not clearly understood. It is quite possible that the same phenomenon also happens on press. In Figures 42 - 57, in the Appendix, these points are shown as empty symbols in the same color as the non-excluded

good points.

- Automated exclusion of force readings once the tack retreat has been detected. In other words, all points past the maximum. These are shown as smaller data points in a lighter tone.
- Automated notation on the chart of the maximum force point. These are large symbols with a light-colored interior.

2.8 The Measurements and Modeling of Coating Porous Structure

The increasing emphasis on ink-coating interactions as a function of pore characteristics has resulted in multiple measuring and modeling methods to simulate the porous structure of the coated paper. Schölkopf, Gane and Ridgway [30] classified three primary experimental procedures according to liquid imbibition, permeation and intrusion.

- Digital image analysis and electron microscopy.

Digital image analysis and electron microscopy can provide a reliable digitized micrograph of the cross-section of coated papers. The atomic force microscope (AFM) can provide a 3-D image on both the micro- and nano-scale. This technology has been used to study paper and print topography [15, 52, 53]. The Scanning Electron Microscope (SEM), operated in secondary electron images (SEI) mode, allows an extremely detailed analysis of the distribution, local composition and structure details of a coating layer [26, 54, 55], but the sampling is critical due to the accuracy of the micrograph. A suitable procedure was introduced by Chinga *et al.* [54]. However, SEM has limited depth of resolution, which does not enable the detection of features much less than 1 μm, especially in the height direction. In addition, the high voltage required for higher magnifications with high resolution may

cause damage to the paper surface.

- Mercury intrusion/extrusion porosimetry

Mercury porosimetry has been widely used in the lab and industry to characterize the porous structure of samples. It generates the data based on Washburn's equation which indicates that the pressure forces a non-wetting liquid to enter a capillary of circular cross-section is inversely proportional to the diameter of the capillary and directly proportional to the surface tension of the liquid and the cosine of the contact angle on the solid surface [56]. Assuming that the pore is a right circular cylinder, thereby the incremental volume of mercury and associated pressure (pore size) values yield a table of pore size intervals and incremental volumes associated with each interval. The sophisticated design allows the mercury porosimetry to be applied over a capillary diameter range from 0.003 μm to 360 μm (five orders of magnitude) and provide a good indication of the various characteristics of the porous structure [57].

However, this method has its own disadvantage, such as the assumption of pore shape and the shielding effects. Thus, it is usually applied in combination with a pore-network simulator, such as Pore-Cor modeling software [59].

- Modeling methods

With the development of computer technology, numerical approaches have been proposed to model coating structure. They were introduced and compared by Vidal and Bertrand [58], which have recently been applied in the coating literature or have the potential for use in future research. For example, a mature modeling software Pore-Cor is most widely used on the study of coating structure recently [59]. It can interpret mercury intrusion or/and water retention curves to devise three-dimensional pore geometries via pore-throat connectivity [59].

CHAPTER III

EXPERIMENTAL

3.1 Coating Formulation

Two commercial SC (before calendaring) $CaCO_3$ filled wood-containing papers (higher filled-A and less filled-D) were used as the base papers. Two pigments, coarse $CaCO_3$ (CC) and ultrafine $CaCO_3$ (UF), were chosen to create coatings of different pore structures. Two styrene-butadiene (SB) latexes of different polarities, but similar glass transition temperatures (T_g), minimum film formation temperatures (MFFT) and particle size were used as binders. The use of acrylonitrile as a copolymer in HPL01 imparts a higher polarity to the polymer surface and is intended to present more polar surface energy forces at coating surfaces. The properties of the binders, according to the manufacturer, are given in Table 2.

Table 2

The characteristic of two SB latexes

Latex	**Polarity**	**pH**	**Solids %**	**Particle Size (nm)**	**MFFT (℃)**	**T_g (℃)**	**Acrylonitrile modified**
LPL01	Low	5.5	49	130	6.0	5	No
HPL01	High	6.5	50	110	9.4	9	Yes

A series of coating formulations were prepared according to Table 3. This is a three variable, two-level full factorial design. The product information for the

pigments is shown in the Appendix (Table 14). The solids of the coatings were adjusted to about 64% and the pH values were adjusted to approximately 8 by use of ammonia. The same percentage of carboxymethyl cellulose (CMC) thickener was added to each coating to assure similar Hercules high shear viscosities. The Brookfield viscosities of the coatings were measured at 100 rpm using a # 4 spindle at 25℃.

Table 3

Coating formulations (Dry parts)

Coating #	CC	UC	HPL01	LPL01	CMC
1	100	0	8	0	1.5
2	100	0	12	0	1.5
3	100	0	0	8	1.5
4	100	0	0	12	1.5
5	30	70	8	0	1.5
6	30	70	12	0	1.5
7	30	70	0	8	1.5
8	30	70	0	12	1.5

The coatings were blade coated on a Cylindrical Laboratory Coater (CLC) to obtain a coat weight of 8 g/m^2. To maintain the pore structure of coatings, and avoid additional process variability, the coated papers were not calendered.

3.2 Characterization of Base Papers and Coated Papers

The properties of all papers were measured under the guidance of TAPPI Standard Methods with different instruments (Table 4).

Table 4

TAPPI Standards and instruments for the paper properties measurements

Paper Properties	**TAPPI Standard Methods**	**Instruments**
Basis Weights (g/m^2)	T401	SMART system 5 (CEM)
Ash Contents (525 ^{0}C) %	T413	Furnace
Ash Contents (900 ^{0}C) %	T211	
Brightness (%)	T452	Brightimeter MICRIO S-5 (Technidyne)
75°gloss (%)	T480	75°Gloss (Technidyne Profile/Plus)
Thickness μm)	T411	Thickness (Technidyne Profile/Plus)
Roughness (μm)	T555	Parker Print Surf (PPS) Tester
PPS Porosity (mL/min)		
Absorbency Curves Contact Angle Surface Energy	/	First Ten Angstroms Dynamic Contact Angle Measurement System (FTA 200)
Properties of Pores	/	Mercury Porosimeter (AutoPore IV, Micromeritics)
Ink Setting Rates	/	Deltack Printability Tester (Prüfbau)

The PPS roughness was measured by using soft backing and clamping pressure 1000 kPa to simulate the offset press. When measuring the PPS air permeability, the clamping pressure was set at 1000 kPa as well.

The permeability coefficient of each paper was calculated by substituting the PPS porosity Q and the thickness L from the following equation [60]:

$$\text{Permeability Coefficient, K } (nm^2) = 48838 * Q \text{ (ml/min)} * L \text{ (m)} \qquad (1)$$

Where:

Q= PPS permeability of the paper

L= thickness of the paper.

The permeability coefficient K was primarily defined in Darcy's Law [61]:

$$Q = \frac{K A \Delta P}{\mu \Delta L} \qquad (2)$$

Where:

Q = volumetric flow rate

A = cross sectional area

ΔP = pressure drop

μ = fluid viscosity.

Equation (2) was derived by substituting the corresponding parameters with the standard parameters from the PPS tester (Table 5). Because it can be interpreted in terms of an effective capillary cross sectional area of pores, this coefficient can indicate the porous structure in the area unit better than the PPS Porosity in the unit of airflow rate [60].

Table 5

Parameters used to derive the equation for permeability coefficient [60]

Parameters in Darcy's Law	**Standard Parameters on the PPS tester**
Q (volumetric flow rate)	Q (PPS porosity)
ΔL (distance the fluid flow through)	L (thickness of the paper)
A (cross sectional area)	10 cm^2
ΔP (pressure drop)	6.17 kPa
μ (fluid viscosity)	1.80075E-05 Pa s (Ns/m^2) at 23 ℃

Two testing liquids, water and methylene iodide (MI) were used in the FTA dynamic contact angle measurement system. The absorbency curve of each paper was drawn as the sessile drop volume vs. time; meanwhile the contact angle was determined at the equilibrium time. The surface energy of each paper was then approximated by using the Owens-Wendt equation in the FTA software [62].

The mercury porosimetry of each paper was characterized on a Micromeritics

AutoPore IV 9500 Mercury porosimeter. To eliminate the contribution of the base papers, all samples were taped on one side and the data of the incremental intrusion volume of the coated papers were subtracted from those of the base papers at the corresponding pore diameters.

Both the base papers and the coated papers were run on a prüfbau Deltack Printability Tester to detect the ink setting rate profiles. A controlled volume of a roller-stable, quickset testing ink was distributed at 18 ℃, which was monitored and controlled to 0.1 ℃. The samples were printed under an impression pressure of 800 N at a velocity of 0.5 m/s. The splitting forces were measured every 3 s (2 s for double coated papers), between 100 mm and 175 mm on a 200 mm long paper sample, until either serious coating picking was observed or ink setting slowed from its maximum tack. The forces and time at "coating failure" were recorded by punching "P" on the keyboard once picking appeared on the ink wheel.

CHAPTER IV

RESULTS AND DISCUSSION

4.1 The Properties of Base Papers

The basis weight, the filler contents and thickness of the base papers are listed in Table 6. The ash contents were measured at 525℃and 900℃ to determine the level of $CaCO_3$ filler within the two base papers,.

Table 6

The basis weights, filler levels and thicknesses of the two base papers used

Base Paper #	**Basis Weight (g/m^2)**	**$CaCO_3$ Filled Level (%)**	**Thickness (μm)**
A	47.36	11.44	57.2
D	47.27	9.95	57.9

In Figure 15, base paper D shows a higher brightness than base paper A. In Figure 16, the 75° gloss of base paper A is about one unit higher than that of base paper D.

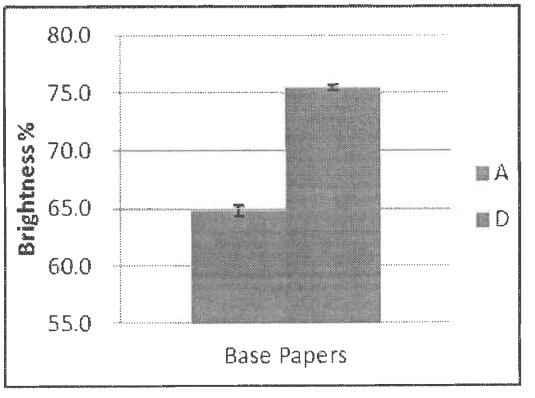

Figure 15: Brightness of base papers

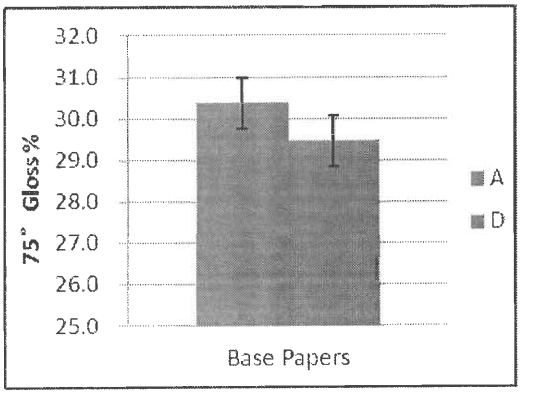

Figure 16: 75° Gloss of base papers

The PPS Roughness of base paper A is slightly higher than that of base paper B in Figure 17.

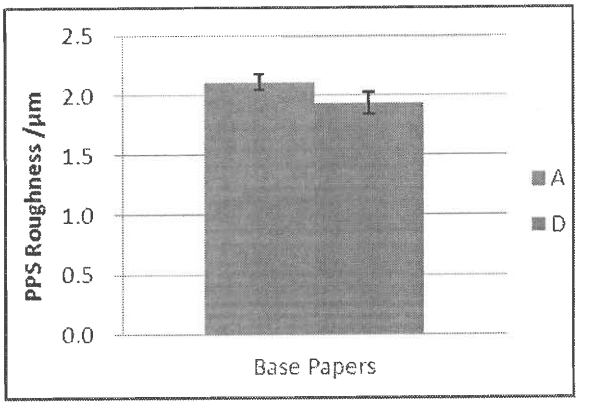

Figure 17: PPS Roughness of the base papers used (CP 1000 kPa/Soft Backing)

As seen in Figures 18 and 19, the PPS porosity of base paper A is much higher than that of the base paper D. The permeability coefficients of the two base papers were calculated by substituting the measured PPS Porosity and thickness values into equation (1). The higher permeability coefficient of base paper A suggests that the liquid can be absorbed faster than that of base paper D.

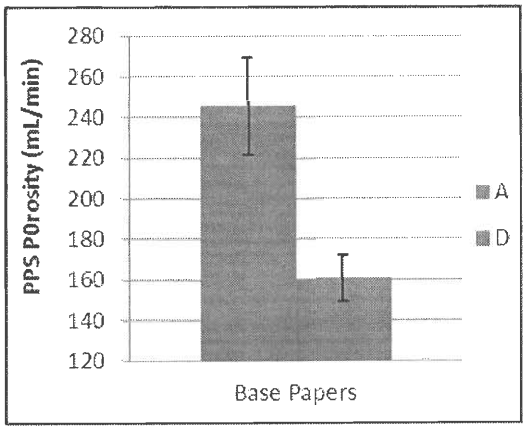

Figure 18: PPS porosity of base papers (CP 1000 kPa)

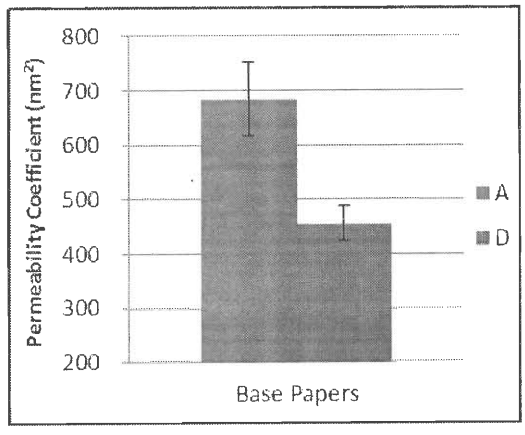

Figure 19: Permeability coefficients of base papers

The prediction from the permeability coefficients agrees with the water and methylene iodide (MI) absorbency results for the base papers in Figures 20 and 21. The water absorbency of the two base papers is very close (A: 2.585 μL, D: 2.538 μL). However, as shown in Figure 21, the difference in absorbency of the two base sheets is significantly different for the non-polar liquid (MI): for the same period of time, the absorptive volume of base paper A (1.431 μL) is higher than that of D (0.957μL).

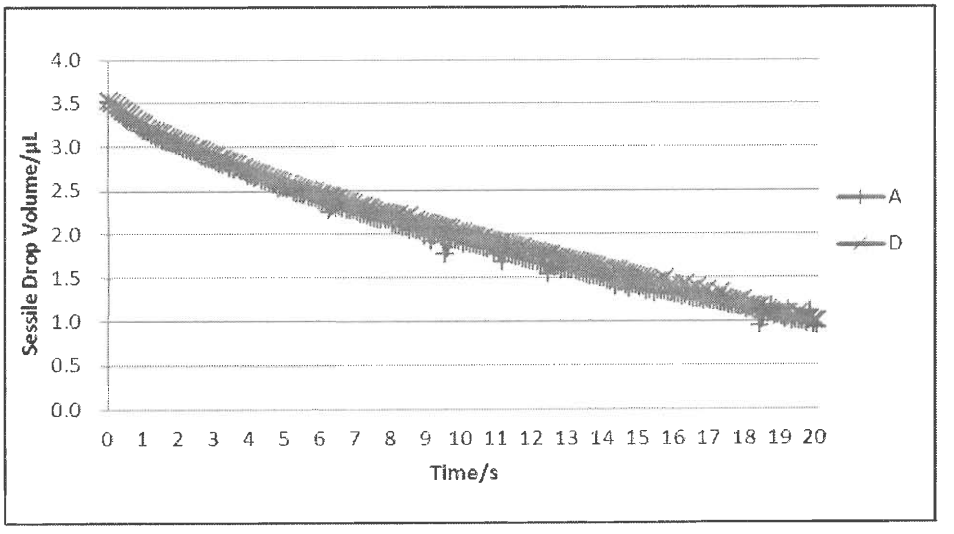

Figure 20: Water absorbency of base papers

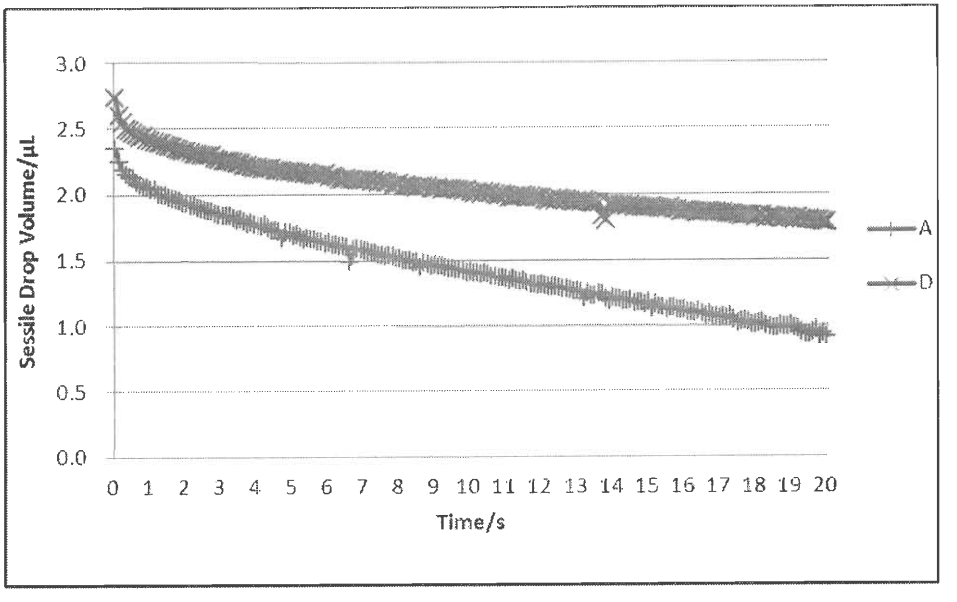

Figure 21: Methylene iodide (MI) absorbency of base papers

Meanwhile, the change in contact angle was also measured. From the contact angle measurements with water and methylene iodide (Fig. 22-23), the equilibrium

drops were observed and used to determine the surface energy of the base papers (Table 7).

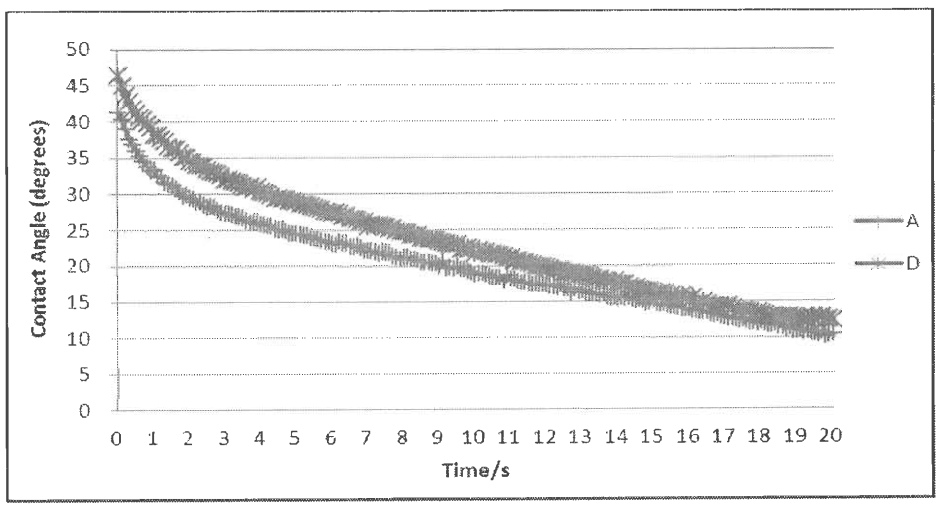

Figure 22: Contact angle of water on the base papers

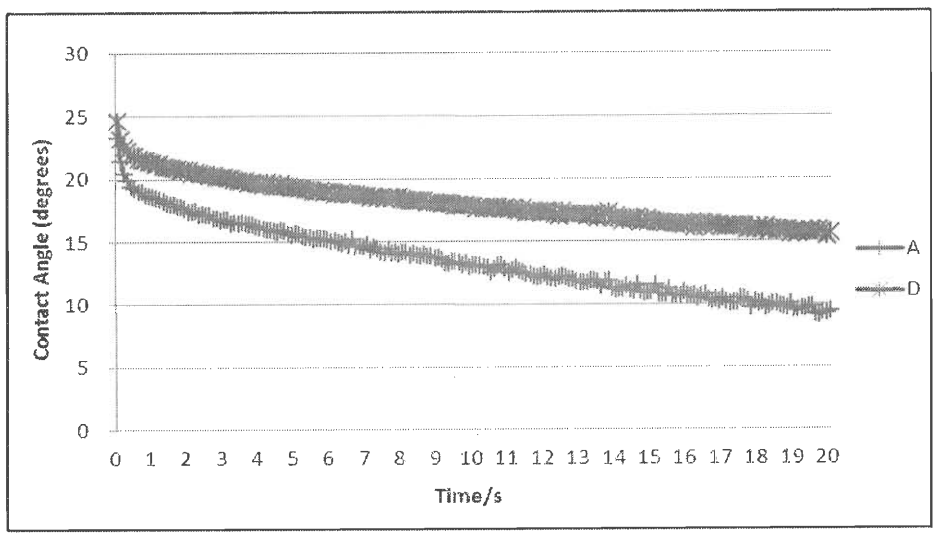

Figure 23: Contact angle of methylene iodide (MI) on the base papers

Table 7

Surface energy of base papers

Base Papers	**A**		**D**	
	Avg.	Std.	Avg.	Std.
Surface Energy(dynes/cm)	79.56	0.161	78.47	0.474
Dispersive Component	50.11	0.108	48.73	0.320
Polar Component	29.45	0.161	29.74	0.475

The ink setting rate profile of the base papers were recorded by using a prüfbau Deltack printability tester (Fig. 24-25). Each test was run in duplicate. For example, the legend "A-01" in the graph thereby reflects the first run and A-02 reflects the second run on base sheet A. From these graphs, the average slope of a best-fit straight line to the build-up portion of the curve, the average picking force and the average passes to fail were found and the results listed in Table 8.

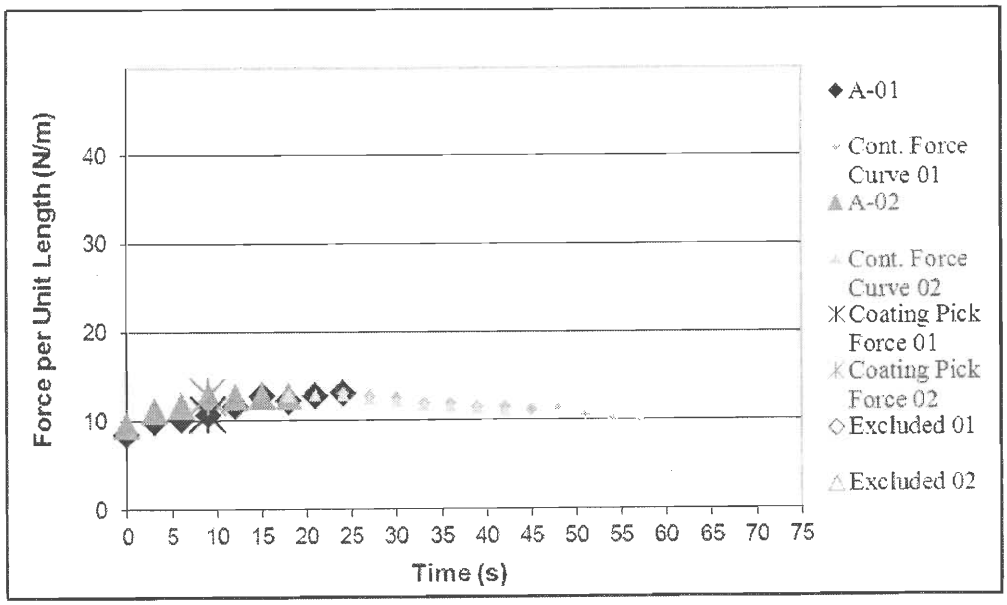

Figure 24: Deltack ink setting rate profile of base paper A

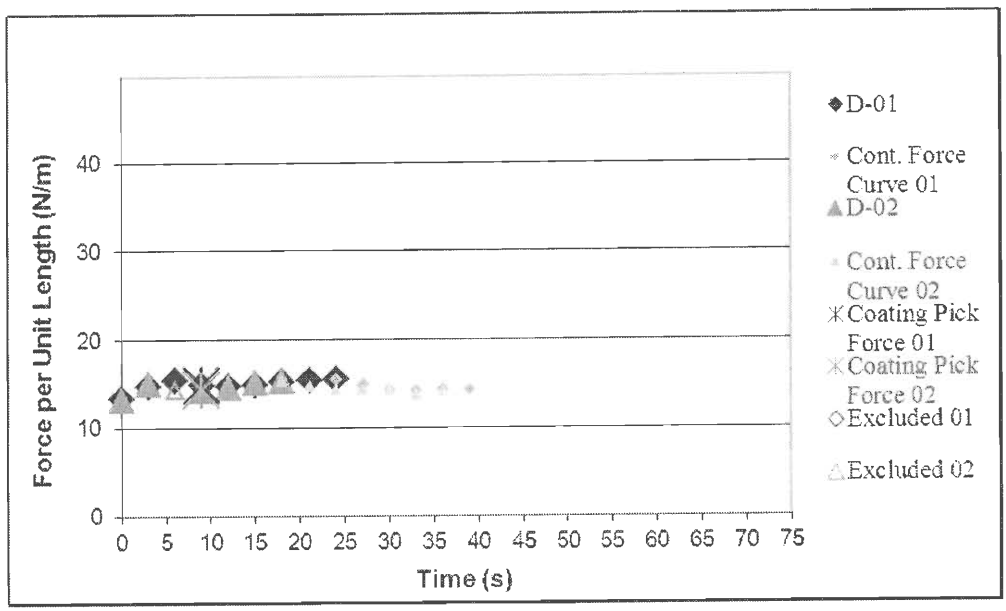

Figure 25: Deltack ink setting rate profile of base paper D

The ink setting rate is defined as the ink splitting force over the time which is

expressed here as the ink setting slope. The picking/failure force is recorded when pick is first seen on the print wheel. The maximum ink tack is detected by an Excel algorithm after importing the data. Maximum forces are plotted as a light orange or light blue inside a dark orange or dark blue point on the force-time graphs. Force-time points to the right of the maximum are colored as light orange and light blue. The passes to failure gives the time from the build-up of ink tack to the failure with the time interval 3s. Since a higher ink setting slope represents a higher ink setting rate, it can be seen in Table 8 that base sheet A sets the ink faster than D which matches the prediction from the permeability coefficient and the liquid absorbency results for the base papers. The picking force of base paper A is slightly lower than that of D when they passed the same time intervals to fail. It was expected that the setting rates of the base papers should be up to at least 0.7 N/m. s to ensure the proper acceleration of ink setting rates when coated.

Table 8

Deltack ink setting slope, picking force and passes to fail of base papers

Base Paper #	**Ink Setting Slope (N/m·s)**	**Picking Force (N/m)**	**Passes to Fail**
A	0.18	11.84	3
D	0.07	14.58	3

4.2 The Properties of Coatings and Single Coated Papers

The coatings were formulated according to Table 3 and the properties of them are shown in Table 9.

Table 9

The properties of the coatings applied

Coating #	Solids %	pH	Hercules Viscosity (centipoise)	Brookfield Viscosity at 100 rpm (centipoise)
1	63.36	8.15	43.3	2160
2	63.46	8.01	39.0	2492
3	63.11	8.17	41.2	2740
4	62.98	8.42	37.2	3768
5	64.14	8.35	46.3	3160
6	64.30	8.25	42.7	3620
7	63.71	7.95	45.6	4380
8	64.11	8.23	42.9	5430

The base papers were coated by blade using a cylindrical laboratory coater (CLC) with the targeted coat weight 8 g/m^2. The actual coat weights and thicknesses obtained are listed in Table 10.

Table 10

The coat weights and thicknesses of the CLC coated papers

Coating #	Base Sheet #	Coat Weight (g/m^2)	Thickness (μm)
1	A	8.1	62.4
	D	7.6	60.3
2	A	8.2	62.3
	D	8.3	59.5
3	A	8.0	62.4
	D	7.8	61.3
4	A	8.2	62.5
	D	7.8	60.2
5	A	8.1	62.3
	D	8.4	61.1
6	A	8.4	62.3
	D	7.7	60.5
7	A	8.4	62.5
	D	8.0	60.0
8	A	7.7	61.9
	D	7.7	59.9

Compared with the brightness of base papers in Figure 15, the brightness of the coated papers was all improved by about 4 units by the coatings (Fig. 26). It is also observed that the brightness of the coated papers D1-D8 is higher than that of A1-A8 due to the higher brightness of the base paper D.

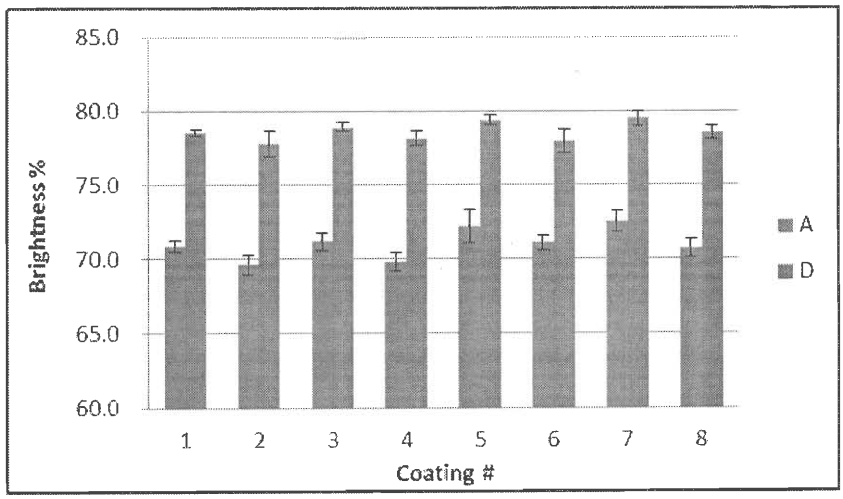

Figure 26: Brightness of coated papers

The 75° gloss of the coated papers is shown in Figure 27. There are no big differences among the two base papers. However, it is obvious that coatings can be grouped into two: the papers with coatings 1-4 have a higher gloss than those with coatings 5-8. It has been stated that the gloss is determined by the topography of the paper, including macro roughness and micro roughness. Considering the roughness of the coated papers in Figure 28, the higher roughness of the papers with coatings 1-4 in some degree resulted in them having a lower gloss. This is probably related to the coatings 1-4 only containing coarse carbonates, which tend to create more open and fewer pores.

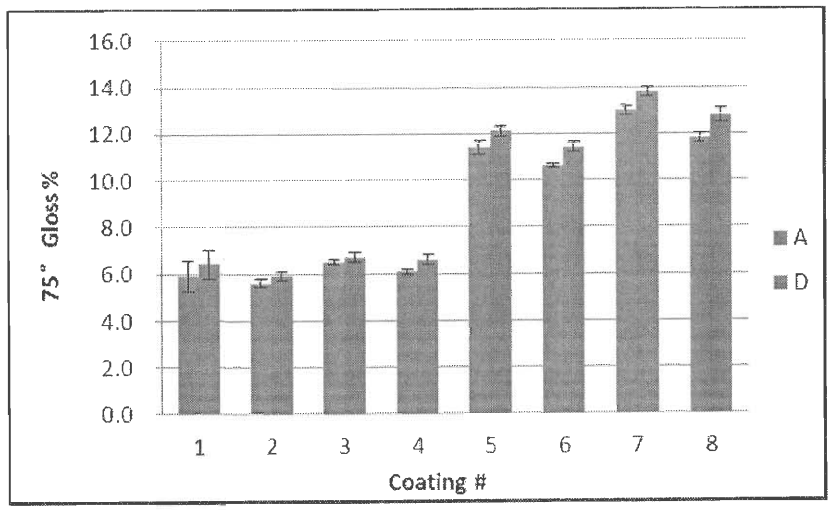

Figure 27: 75° Gloss of coated papers

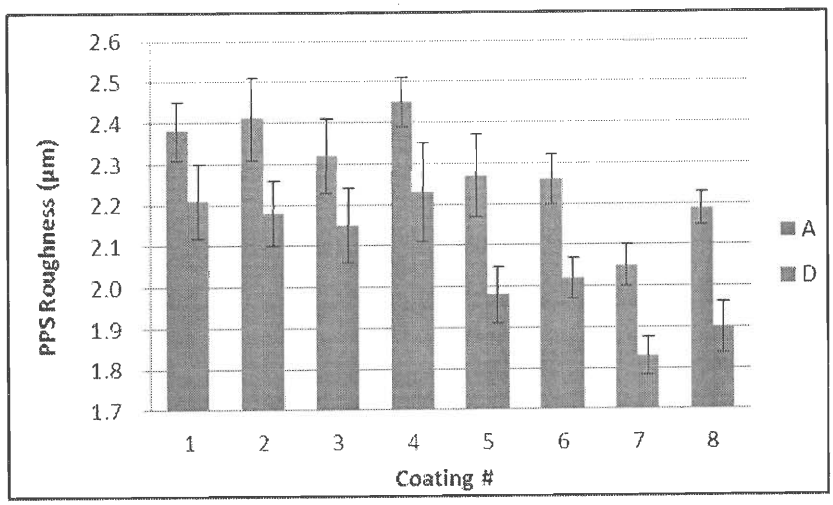

Figure 28: PPS roughness of coated papers

The dynamic contact angle measurements of the coated papers determined by using water and methylene iodide (MI) are shown in Figures 29- 32. The surface energy and polar component of each paper were approximated from theses measurements by the software (Owens-Wendt method [62]) and the results plotted in Figures 33 and34.

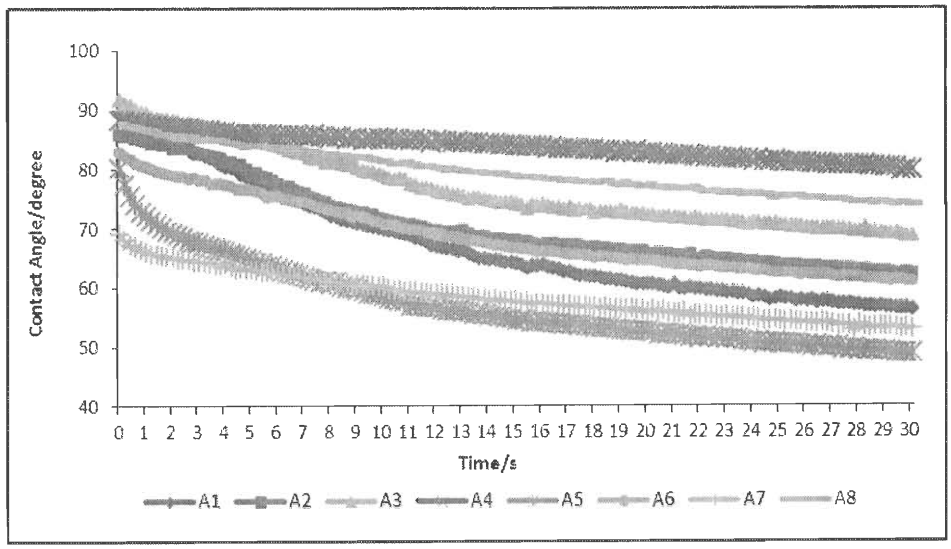

Figure 29: Contact angles of water on the coated papers A1-A8

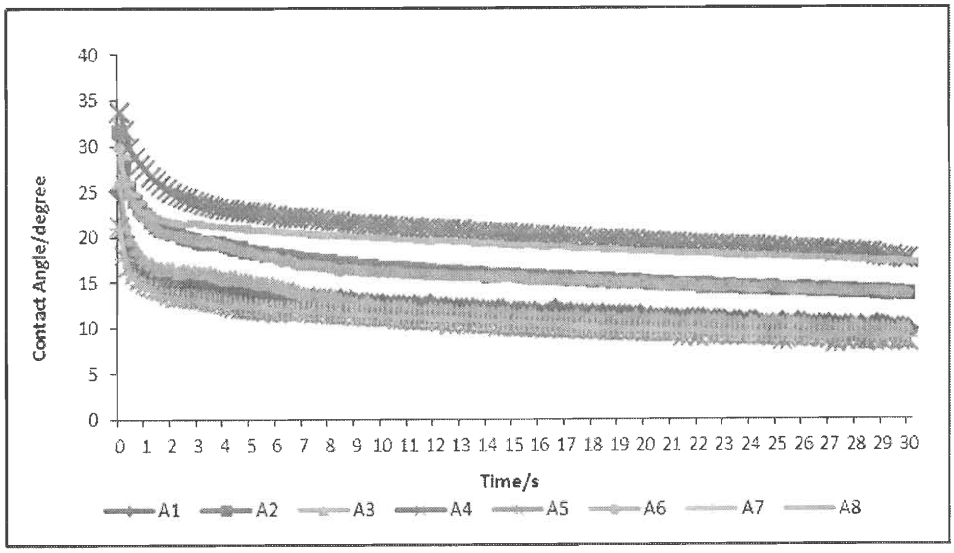

Figure 30: Contact angles of methylene iodide (MI) on the coated papers A1-A8

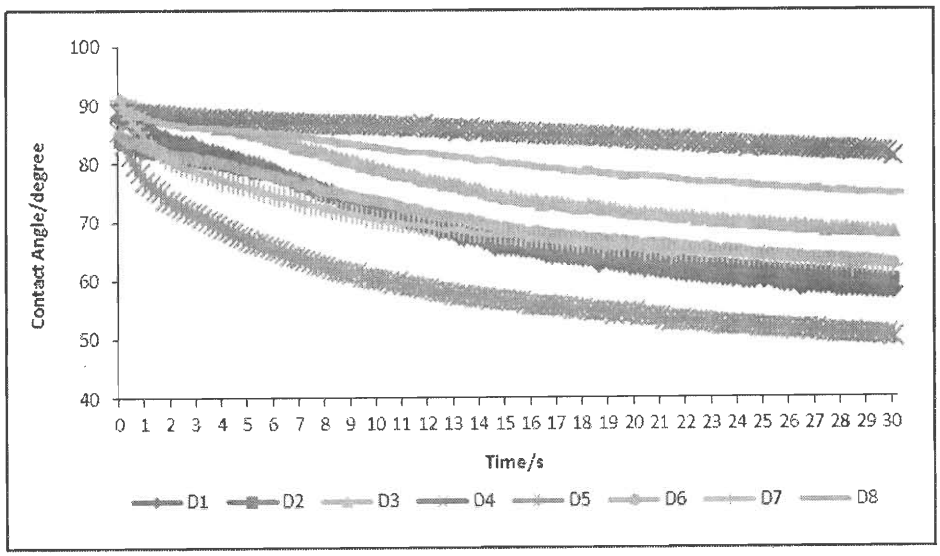

Figure 31: Contact angles of water on the coated papers D1-D8

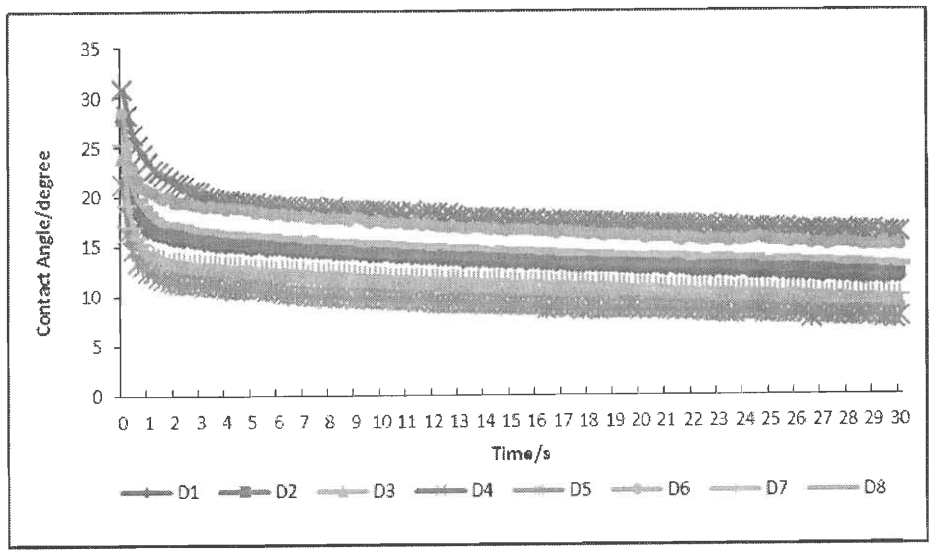

Figure 32: Contact angles of methylene iodide (MI) on the coated papers D1-D8

It turned out that the differences in the polar components of the coating contributed more to the surface energy than that of the dispersive components because of the different latexes of varying polarity being used (Fig. 33-34). The coatings with

the same level of high polarity latex and the same carbonates have higher polar surface energy components as we proposed (coatings 1&3, 2&4, 5&7, 6&8). However, it is shown in Figure 34 that the lower level of the same type of latex and carbonates resulted in higher polar components. These findings are important because the surface energy and polarity of a coating can affect ink setting [63-65].

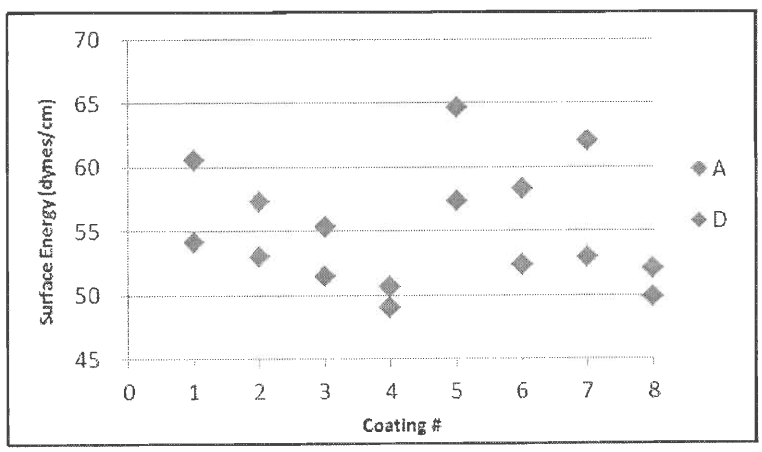

Figure 33: Surface energy of coated papers

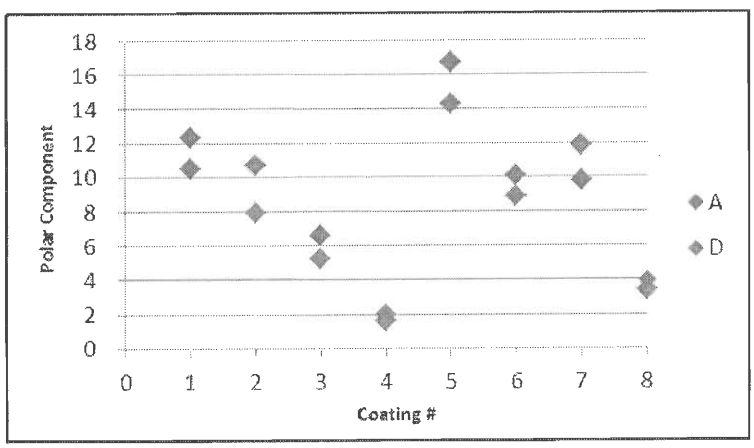

Figure 34: Polar components of coated papers

The permeability coefficients and mercury intrusion curves were used to determine the properties of the coating porous structure. It should be noted that neither of them can provide the full information about the coating layer individually, due to the complex porous structure of the coated paper by its nature.

The permeability coefficient obtained from the PPS porosity and paper thickness measurements is only related to the permeable pores in both the coating and the base paper. Moreover, although the measurement of the permeability on the PPS tester simulates the printing nip on the offset press, which is also close to the printing pressure on the Deltack printability tester, this pressure is much lower than the pressure applied during the mercury porosimetry test, the differences between fluid viscosities are also great. Assuming that the pore or capillary is cylindrical and the opening is circular in cross-section, Washburn's equation states that the diameter of a pore is inversely proportional to the pressure and proportional to the fluid viscosity [56]. Therefore, it is not surprising that the results from these measurements are not consistent. In the case of mercury porosimetry, much research has been done to evaluate this measurement and some other compensatory methods, measurements, such as Pore-Cor modeling software, have been introduced. The shortcomings of the mercury porosimetry for instance are that the results cannot detect the shielded pore space so the intrusion curve may misrepresent the volume of the pores at a certain diameter because of the different pressures of mercury required to break into the pore throats and pore cavities [57].

Therefore, the combination of porous structure and surface energy measurements is necessary to indicate the contribution of the porous structure to the resulting Deltack ink setting rate and surface energy to the chemical effect on the ink setting rate.

As shown in Figure 35, the permeability coefficients of all the coated papers were reduced dramatically by the coatings applied to both base papers (A=683.92 nm^2; D=454.97 nm^2). The coatings were designed to create less permeable structures on the top to induce slow ink setting at the beginning and the more permeable structure below it was expected to set the ink fast. The difference in the permeability coefficients of base papers are also shown here with base paper A being a little more permeable than D.

By comparing the permeability coefficients of the coated papers for the same base paper, we see the contrast of the porosity of the coating layers. The papers coated at the lower latex level with the same pigment and latex type (coatings 1, 3, 5, 7) generated higher permeability coefficients in comparison with the others (coating 2, 4, 6, 8). This means that the higher level of latex reduced the permeability coefficients, by filling the porous structure of coatings. It is surprising that the different particle size carbonates did not show a dramatic effect on the permeability coefficients when comparing coatings 1&5, 2&6, 3&7, 4&8. Neither did the latex polarity (coatings 1&3, 2&4, 5&7, 6&8).

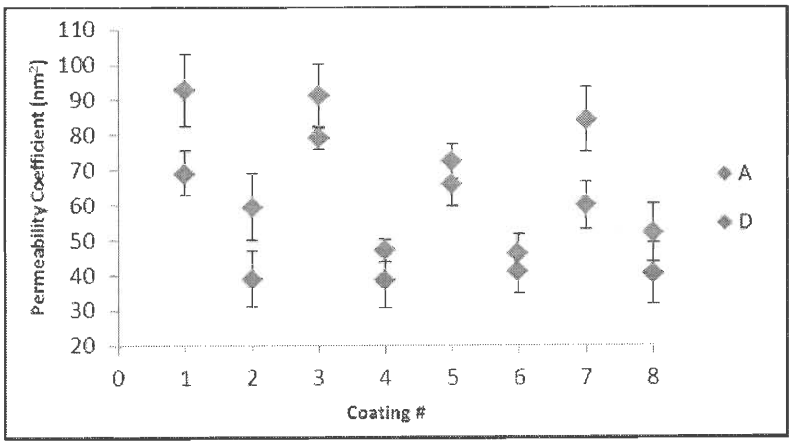

Figure 35: Permeability coefficients of coated papers

It is well-known that the incremental pore volume in the graph of Mercury Incremental Intrusion vs. Pore Diameter (Fig. 36, 37, 39, 40) is the detected volume of pores (or pore number) at a certain diameter. In other words, the larger area under the curve, the more pores exist at a certain diameter, which can also be expressed as pore density (pore number per unit area). As mentioned before, both the pore size and the pore density determine the ink setting rates of papers and the coatings with high polarity of latex are expected to set ink more slowly. To illustrate the porous structure of the coating layer, the incremental intrusion volume of each coated paper was subtracted by that of the base paper and the pore diameters in the graph were limited within 0μm to 1μm, which is believed to limit the range of the pores in the coating layer.

The pore size distribution curves in Figure 36 are from the papers coated with coarse carbonates and Figure 37 shows the curves of the coated papers containing the fine/coarse carbonates blend. It is observed that the coated papers A5-A8 have more fine pores while the coated papers A1-A4 have more pores of larger size. The combination of these properties with the findings in Figures 33-34, are the cause for

the ink setting of coated papers A1-A4 being slower than A5-A6 (Fig. 38). It is also interesting that the ink setting rate of coated paper A3 is very close to that of A6 and a bit higher than A6 after about 12s. The pore size distributions of these two papers are not persuasive concerning this phenomenon, but the higher permeability coefficient (Fig. 35) and lower polar surface energy component (Fig. 34) of coated paper A3 can account for this finding.

In Figure 36, coated paper A1 has more pores with diameters in the range from 0.24μm to 1.0μm than coated paper A2. This corresponds with the air permeability coefficients in Figure 35. The ink setting on A1 thereby is faster than A2, though the polar surface energy component of A1 is higher than A2 (Fig. 34). Compared with coated paper A4, the pore density of coated paper A3 seems a little higher, which also matches the air permeability coefficient results (Fig. 35). Thus, A3 sets ink faster than A4, even though it has a higher polar surface energy component (Fig. 34).

Comparing the pore size distribution curves of coated paper A5 with A6, they are very close between the diameter range of 0μm and 0.25μm, although A5 shows slightly more pores from 0.1μm to 0.25μm. Between the diameters 0.25μm to 0.6μm, A6 has a bit more pores than A5. Considering that the permeability coefficient of coated paper A5 is 25 units higher than that of A6 (Fig. 35), this result may explain why coated paper A5 sets the ink faster than A6 despite A6 having a higher polar surface energy component (Fig. 34). Such analysis can similarly be applied to the differences in ink setting rates for coated papers A7 and A8.

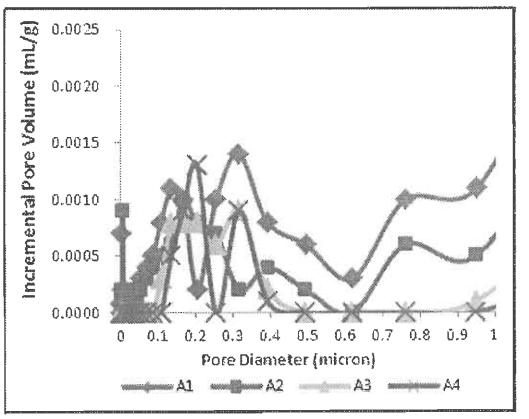

Figure 36: Pore size distribution in the coating pores diameter region of coated papers A1-A4

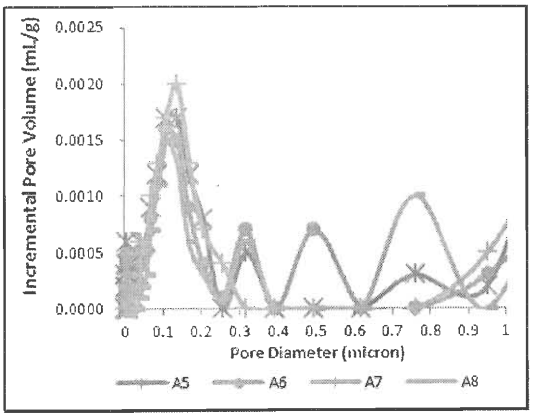

Figure 37: Pore size distribution in the coating pores diameter region of coated papers A5-A8

From the above discussion, the effects of latex level on the permeability coefficients and the pore size distributions of the coatings in turn on the ink setting rates are seen. Moreover, in Figure 38, the coated papers with the same type of pigment and the same level of latex, but higher polarity, set the ink slower in terms of coated paper A1&A3, A2&A4, A5&A7 and A6&A8.

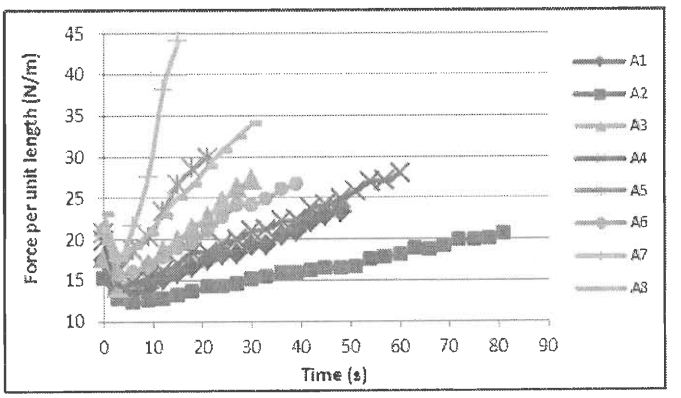

Figure 38: Deltack ink setting rate profile of coated papers A1-A8 from the beginning to the maximum tack point

The contrast of the pore size distributions of coated papers D5-D8 with D1-D4 in Figures 39 and 40 obviously demonstrates that the coating with fine carbonates create a larger number of smaller pores than those with coarse carbonates. Combining these results with the higher surface energy and polar components found in Figures 33 and 34, the ink setting curves of coated papers D5-D8 are higher than those of coated papers D1-D4, as shown in Figure 41.

In Figure 39, the pore size distribution curves all clearly lie in three pore diameter regions: 0.007μm-0.5μm that is near the maximum pressure, is believed to be caused by the mercury filling the void in the sample cup produced by the collapse or compression of the sample material [56]. The porous differences are shown in the other two diameter regions. The coated paper D3 has the highest pore density with diameters from 0.007μm to 0.5μm, but the lowest pore density between 0.75μm to 1.0μm diameters, which corresponds to it having the largest permeability coefficient among coated papers D1-D8 (Fig. 35). Combining these results with the contribution of the low polarity latex, it is not surprising that coated paper D3 set the ink the fastest among the D1-D4 coated papers (Fig. 41). As such, the slowest ink setting of coated

paper D2 can be explained by it having the smallest pore density between the pore diameters from 0.007μm-0.5μm, the lowest permeability coefficient among the D1-D4 coated papers and the addition of the high polarity latex. The pore size distribution curves of D1 and D4 are very similar in the pore diameter region of less than 0.2μm, but coated paper D1 has more pores in the diameter region 0.2μm-0.5μm and fewer pores in the diameter region 0.75μm-1.0μm. Taking their permeability coefficients into consideration (Fig. 35), it is clear why the ink setting rates are close at the beginning of the test up until around 27 s, where D1 then sets the ink faster than D4 (Fig. 41).

The effect of latex level on the pore size distribution of the coated papers D1-D4 is the same as found for A1-A4, which caused the differences of ink setting rates. So is the effect of latex polarity.

Three diameter regions of pore size distribution curves of coated papers D5-D8 also appear in Figure 40. The big differences are seen in the pore diameter regions from 0.05μm to 0.4μm and from 0.76μm to 1.0μm. A comparison of D6 to D5 shows more pores in the diameter region of 0.05μm to 0.25μm but fewer pores in the diameter region from 0.76μm to 1.0μm. The permeability coefficient of coated paper D5 is higher than that of D6 (Fig. 35). Thus, coated paper D5 gave a higher ink setting rate than D6.

In contrast with coated paper D8, D7 has fewer 0.05μm to 0.4μm diameter pores but a bit more pores in the region of 0.76μm to 1.0μm. In terms of their permeability coefficients, D7 resulted in a larger value than D8. Therefore, the ink setting rate of D7 is larger than D8 in spite of its higher polar surface energy component.

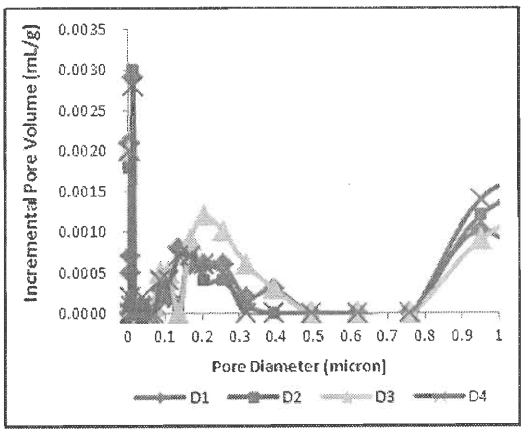

Figure 39: Pore size distribution in the coating pores diameter region of coated papers D1-D4

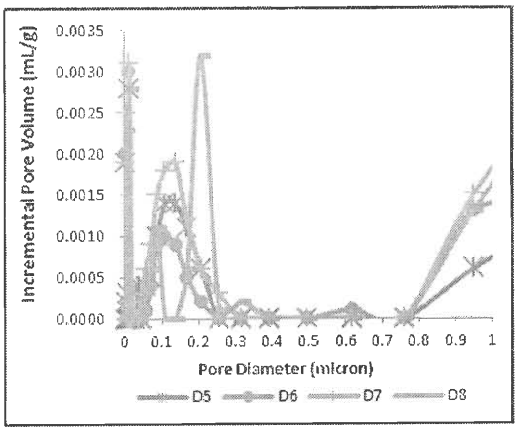

Figure 40: Pore size distribution in the coating pores diameter region of coated papers D5-D8

From the above discussion, the effects of latex level on the permeability coefficients and the pore size distributions of the coatings in turn on the ink setting rates are again observed for coated papers D1-D8. The influence of latex polarity is also observed in Figure 41 by comparing the ink setting of the coated papers with the same type of pigment and level of latex, but different polarity (A1&A3, A2&A4, A5&A7 and A6&A8).

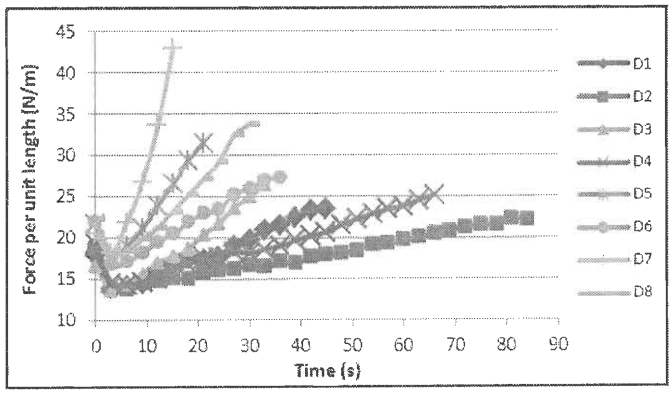

Figure 41: Deltack ink setting rate profile of coated papers D1-D8 from the beginning to the maximum tack point

In summary, the influence of carbonates with different particle sizes was seen in the pore size distribution curves and the permeability coefficients, which explained the difference in the ink setting rates. The influence of latex level has also been observed, which can be explained by the filling of pores. The effect of a higher latex polarity on the surface energy and polar component was found, as expected, to set the ink slower. However, for the same latex type, the amount of latex used was not as significant as the other factors.

4.3 Statistical Analysis of Ink Tack Build Slope and Coating Failure Force

A 3-variable 2-level statistical study of ink tack slope build was carried out in Minitab to provide the relative power of each independent variable on the affect the slope, Table 11. The original statistical analysis is attached in Appendix (Table 15). The results indicate that the pigment type is significant with up to 99.5% confidence. The level of latex ranked second in significance with 98.7% confidence while the polarity of latex is significant with 97.1% confidence. Only the type of base paper is not significant to the slope which can attributed to either the low ink setting slopes of

the base papers or the low contribution of their properties to the ink setting of the coated papers. Therefore, the selection of the base sheet should be considered further.

Considering the main effects of the three variables, the pigment type results in a slope range of 0.7238 N/m·s (mean of slopes for fine/coarse pigment blend – mean of slopes for coarse, which is twice the slope of the corresponding linear regression curve). The latex level is next, with a slope range of 0.6063 N/m·s (mean of slopes for 8 parts – mean of slopes for 12 parts) and the latex type is third with a slope range of 0.5112 N/m·s (mean of slopes for low polarity – mean of slopes for high polarity). The type of base paper is the last that shows 0.0538 N/m·s (mean of slopes for base paper A – mean of slopes for base paper B). The linear regression model only gives an R^2 value of 71.69% and adjusted R^2 value of 61.39%.

Table 11

Minitab statistical analysis of 3-variable 2-level study of ink tack build slope on coated papers

Code	Variables				Response
	Base Paper	**Pigment Type**	**Latex Level**	**Latex Type**	
	1: A -1: D	1: Fine/coarse blend -1: Coarse	1: 8 parts -1: 12 parts	1: High polarity -1: Low polarity	**Ink Tack Build Slope (N/m·s)**
A1	1	-1	1	1	0.22
A2	1	-1	-1	1	0.11
A3	1	-1	1	-1	0.52
A4	1	-1	-1	-1	0.24
A5	1	1	1	1	0.78
A6	1	1	-1	1	0.33
A7	1	1	1	-1	2.33
A8	1	1	-1	-1	0.61
D1	-1	-1	1	1	0.23
D2	-1	-1	-1	-1	0.11
D3	-1	-1	1	1	0.43
D4	-1	-1	-1	-1	0.17
D5	-1	1	1	1	0.78
D6	-1	1	-1	-1	0.32
D7	-1	1	1	1	2.06
D8	-1	1	-1	-1	0.61
P-value	0.797	0.005	0.013	0.029	
Main Effect	0.0538	0.7238	0.6063	-0.5112	

From the results, the highest slope should have been obtained for either the A7 or D7 coated papers containing the fine/coarse pigment blend and low level of low polarity binder. The largest slope is indeed found 2.33 N/m·s for A7. As such, the coated paper with the lowest slope should be either coated paper A2 or D2 containing only the coarse pigment and high level of high polarity latex. With a slope of 0.11

N/m·s, both of them are indeed found.

The coating failure force responses were also analyzed statistically (Table 12). The original statistical analysis is attached in Appendix (Table 16). Both the pigment type (100% confidence) and the latex type (100% confidence) showed significant effects. The type of base paper is not significant. Surprisingly, the latex level was also significant, but this should not be construed as a general case. Pigment size exhibited a main effect of 3.775 N/m with the fine/coarse pigment blend being stronger than the coarse pigment. This is a movement of about 20% compared to the mean force reading of the latter coatings 20.4 N/m. The lower polarity latex yielded higher forces with a main effect of 3.500 N/m, a 17% move. The linear regression model gives an R^2 value of 84.95% and adjusted R^2 value of 79.48%.

The papers with the highest dry strength by this pick force measurement (27.5 N/m) were A7 and D7 composed of fine/coarse pigment blend, low polarity latex and higher latex level. Also, interestingly the secondary high strength coating was #8 (failure force of A8 is 25.7 N/m and failure force of D8 is 26.3 N/m). This coating was also made from the fine/coarse blend with low polarity latex but at the lower 8 parts of latex. However, when comparing the passes to failure of coating 8 (Fig. 49, 57) with coating 7 (Fig. 48, 56) on both base papers, it is observed that it took 6-7 passes for the slower #8 to reach the force at which picking first occurs and only 3 passes for #7. Thus, the coating 8 was noted to have exhibited a more promising force-time profile.

Table 12

Minitab statistical analysis of 3-variable 2-level study of coating failure force on coated papers

Code	Variables				Response
	Base Paper	Pigment Type	Latex Level	Latex Type	Coating Failure Force (N/m)
	1: A -1: D	1: Fine/coarse blend -1: Coarse	1: 8 parts -1: 12 parts	1: High polarity -1: Low polarity	
A1	1	-1	1	1	19.2
A2	1	-1	-1	1	18.4
A3	1	-1	1	-1	23.4
A4	1	-1	-1	-1	22.4
A5	1	1	1	1	22.0
A6	1	1	-1	1	21.1
A7	1	1	1	-1	27.5
A8	1	1	-1	-1	25.7
D1	-1	-1	1	1	19.8
D2	-1	-1	-1	1	19.8
D3	-1	-1	1	-1	20.5
D4	-1	-1	-1	-1	19.8
D5	-1	1	1	1	21.1
D6	-1	1	-1	1	23.0
D7	-1	1	1	-1	26.8
D8	-1	1	-1	-1	26.3
P-value	0.631	0.000	0.485	0.000	
Main Effect	0.325	3.775	0.475	-3.500	

4.4 The Selection of Promising Coated Papers

In order to select the coated papers matching the desired ink setting profile, the slopes of first two passes (6 s) and those of the following passes were calculated and listed in Table 13.

Table 13

The evaluation of Deltack ink setting profiles of all coated papers

Sample	Slope <6 s N/m·s	Slope >6s N/m·s	Slope Delta N/m·s	Excluded	Coating Failure Force N/m	Passes (Intervals) to Failure	Promising Graph?
A1	0.125	0.221	0.096	1	19.2	11	
A2	0.091	0.104	0.013	2	18.4	21	
A3	0.353	0.529	0.176	1	23.4	8	Yes
A4	0.118	0.240	0.122	1	22.4	13	
A5	0.588	0.722	0.133	1	22.0	4	
A6	0.180	0.337	0.157	1	21.1	7	
A7	1.667	1.999	0.332	1	27.5	3	
A8	0.462	0.598	0.136	1	25.7	6	Yes
D1	0.095	0.230	0.135	1	19.8	10	
D2	0.248	0.101	-0.146	2	19.8	20	
D3	0.331	0.464	0.132	1	20.5	7	Yes
D4	0.118	0.171	0.054	1	19.8	13	
D5	0.565	0.760	0.196	1	21.1	3	
D6	0.221	0.300	0.079	1	23.0	7	
D7	1.431	3.008	1.577	1	26.8	3	
D8	0.286	0.694	0.408	1	26.3	7	Yes

The graphs of the Deltack ink setting rate profiles on all the coated papers are attached in the Appendix (Fig. 42-57). Given the results in Table 13 and the graphs of ink setting rate profiles, coated papers A3, A8, D3, and D8 are promising. Since the base paper had little impact on the ink setting, coatings 3 and 8 can be considered to fit a more "ideal" approach, but not dramatically enough to be of commercial value. The slope of Coating 3 (Fig. 44 and 52) increases quickly (the first three force points up to 6 s) on both base papers of 0.353 N/m·s and 0.331 N/m·s, which accelerated to 0.529 N/m·s and 0.464 N/m·s, respectively. This coating consists of the coarse pigment with a lower level of the low polarity latex. Coating 8, consisting of the

fine/coarse pigment blend with 12 parts of the low polarity latex, (Fig. 49 and 57) was even more interesting, with slopes of 0.462 and 0.286 N/m·s increasing to 0.598 N/m·s and 0.694 N/m·s, respectively. Since both coatings survived picking until the 7^{th} print cycle (21 s) they are considered robust enough to survive a commercial multi-unit sheet-fed print run.

CHAPTER V

CONCLUSIONS

The coatings with different pigments, binder types and binder levels were applied on two different base papers to create different surface energy, permeability coefficients and pore size distributions. The influence of carbonates with different particle sizes was seen in the pore size distribution curves and the permeability coefficients, which explained the differences in ink setting rates observed. The influence of latex level was also observed, which changed the number of open pores in the coating. The effect of latex polarity on surface energy and polar contribution of the surface energy term was found as expected, and the low polarity latex was found to set the ink slower. However, with the same type of latex, though the polar surface energy components may be different due to the difference in latex level used, its impact on the ink setting is not as significant as the other factors.

The test results from ink tack measuring instrument demonstrated that it has the ability to repeatedly measure force-time curves of ink setting down to 3s at a print speed of 0.5 m/s.

The statistical analysis of the slopes of the force-time curves enabled differences in the contribution of base paper, pigment type, latex level and latex polarity on ink setting to be determined. Except for the type of base paper used, the other factors were all significant to the ink setting slope. The highest ink setting slope was found for the coating containing the highest percentage of fine pigment, lowest level of binder addition and binder of lowest polarity.

The coating failure force responses showed no significant effect from latex

level used, but this should not be construed as a general case. Pigment size and latex polarity had a great influence on coating failure force. The highest dry strength was observed for the coatings prepared from the fine/coarse blend with low polarity latex. The fine/coarse coating with lower parts low polarity latex also exhibited a promising force-time profile (early acceleration of splitting force). The failure forces of these coatings were very similar, but the coating containing less latex failed at a higher number of passes. This is due to the slower ink tack build rate for this coating.

The purpose of this study was to identify coatings showing slow to fast ink setting rates was basically achieved. Such detailed interpretation of tack rise inflection, as a function of coating composition together with insight provided by surface energy and permeability measurements may provide novel insights into the ink setting process. It is anticipated that this approach will support the development of coated paper that is more suited to the rigors of multi-unit sheet-fed printing with

BIBLIOGRAPHY

1. Smith, D.A., Desjumaux, D., Kessler, H.H., Nicolas, N.R., Sharman, S. and Wright, A. (2004): "Operational principles and sensitivity of a new instrument designed to measure and explore offset ink tack dynamics, substrate failure and ink transfer mechanisms" , Proceedings of International Printing and Graphic Arts Conference, Vancouver, Canada.

2. Gane, P., (2000): "Coating structure: advancing coating design for the print media of today and the challenges of the future", 2000 Paper and Coating Chemistry Symposium, Stockholm, Sweden.

3. Chen, T., Joyce, Joyce, M., Smith, D.A., and Fleming, P.D. (2012): "Influencing the inflections in quickset ink setting profiles to improve sheet-fed print quality & efficiency" Proceedings of TAPPI PaperCon, New Orleans, United States.

4. Offset Lithographic Printing Process (2011). Retrieved June 12, 2012, from http://www.pneac.org/printprocesses/lithography/moreinfo2.cfm

5. IMERYS Technique Guides: "Coatings for offset lithography".

6. Kipphan, H. (Ed.) (2001): "Handbook of Print Media" Springer-Verlag Berlin Heidelberg, DE.

7. Sheet-fed Press (2011). Retrieved June 12, 2012 , from http://desktoppub.about.com/cs/printing/g/sheetfedpress.htm

8. Offset Printing (2012). Retrieved June 4, 2012, from http://en.wikipedia.org/wiki/Offset_printing#Sheet-fed_litho

9. Savastano, D. (2007):"The challenges of emulsification: for offset printers, emulsification, or ink/water balance, is a major challenge, and ink companies are offering guidance to help customers run their presses as smoothly as possible". June 4, 2012, from http://findarticles.com/p/articles/mi_hb3143/is_8_13/ai_n29370660/?tag=content;col1

10. Fleming, D. (2011): "Printing inks", WMU course GPS 5201 Handouts.

11. Offset Ink: Basics (2011). Retrieved June 13, 2012, from http://www.ankeetarts.com/Resource_Centre/Offset%20Inks%20-%20Basics.pdf

12. Esa Lehtinen (Ed.) (2000): "Pigment coating and surface sizing of paper", Fapet Oy, Helsinki.

13. Rousu, S., Gane, P. and Eklund, D. (2001): "Influence of coating pigment chemistry and morphology on the chromatographic separation of offset ink constituents", 12th Fundamental Research Symposium, FRC-Oxford, UK.

14. Don Ventresca (2011): "Synthetic binders", WMU Coating Short Course.

15. Ström, G. R., and Karathanasis M. (2007): "Relationship between ink film topography and print gloss in offset prints on coated surfaces", Nordic Pulp &Paper Research Journal, 23(2), p. 156-163.

16. Swan, A. (1973):"Carry-over ink piling on litho presses", Printing Equipment & Materials, 10(113), p. 32-3.

17. Lepoutre, P., DeGrace, J. H., and Mangin, P. J. (1979):"Printability of coated papers and influence of coating absorbency", TAPPI Journal, 62(5), p. 33-36.

18. Franklin, A. T., (1980):"Paper/ink/Press relationships", Professional Printer, 24(2), p. 2-5.

19. Ström, G., Gustafsson, J., and Sjölin, K., (2000): "Separation of Ink Constituents During Ink Setting on Coated Substrates", 2000 TAPPI International Printing and Graphic Arts Conference Proceedings, p. 89 – 99.

20. SPPI (2012). Retrieved June 13, 2012, from http://www.slideshare.net/SappiHouston/ink-setting-and-back-trapping

21. Rousu, S., Gane, P., Spielmann, D., and Eklund, D. (2000): "Separation of offset ink components during absorption into pigment coating structure", 2000 Paper and Coating Chemistry Symposium, Stockholm, Sweden.

22. Xiang, Y., Bousfield, D. W. (2000):"The influence of coating structure on ink tack development". Journal of Pulp and Paper Science, 26, p. 221-227.

23. Xiang, Y., Bousfield, D. W. (2003):"Coating pore structure change after printing", 2003 TAPPI Spring: Advanced Coating Fundamentals Symposium.

24. Xiang, Y., Bousfield, D. W., Hayes, P. C., and Kettle, J. (2004):"A model to predict ink-setting rates based on pore-size distribution", Journal of Pulp and Paper Science, 30(5), 117-120.

25. Kishida, T., Azuma, K., Fukui, T., and Kanou, S. (2001):"Influence of coating pore structure and ink set property on ink dryback in sheet-fed offset printing", 2001 Coating Conference Proceedings.

26. Donigian, D. W., Wise, K. J., & Ishley, J. N., (1996) "Coated Pore Structure and Offset Printed Gloss", TAPPI Coating Conference Proceedings, p. 39 – 45.

27. Preston, J.S., Elton, N. J., Legrix, A., Nutbeem, C., and Husband, J.C. (2002): "The role of pore density in the setting of offset printing", TAPPI Journal, 1(3), p. 3-5.

28. Gane, P., Matthews, G. and Schölkopf, J. (2000): "Coating imbibition rate studies of offset inks: a novel determination of ink-on paper viscosity and solids concentration using the ink tack force-time integral", 2000 Printing and Graphic Arts Conference, TAPPI press, Atlanta, GA. p. 71-88.

29. Schölkopf, J., Gane, P., Ridgway, C. and Matthews, G. (2000): "Influence of inertia on liquid absorption into paper coating structures", Nordic Pulp and Paper Research Journal, 15(5), p. 422-430.

30. Schölkopf, J., Gane, P., Ridgway, C. (2004): "A comparison of the various liquid interaction radii derived from experiment and network modeling of porous pigmented structures", Colloids and Surfaces A: Physicochem. Eng. Aspects 251 (2004) p. 149-159.

31. Rousu, S., Lindström, M, Gane, P., Pfau, A., Schadler, V., Wirth, T., and Eklund, D. (2002): "Influence of latex-oil interactions on offset ink setting and component distribution on coated paper", 11th International Printing and Graphic Arts Conference Proceedings.

32. Desjumaux, D. M., Bousfield, D. W., Glatter, T. P., & Van Gilder, R. L. (1998): "Dynamics of ink gloss influence of latex type over a range of pigment volume concentration", TAPPI Coating/Papermakers Conference Proceedings, p. 875 – 894.

33. Oittinen, P. (1980):"Surface reflection of coated papers and prints", Proceedings of the 15th advances in printing science and technology conference, Pentech, London, p. 344-372.

34. Drage, P.G., Hiorns, A. G., Parsons, D. J., and Coggon, L. (1999):"Factors governing print performance in offset printing of matte papers", TAPPI Journal, 81(11), p. 175-184.

35. Zang, Y. H. and Aspler, J. S. (1994): "The influence of coating structure on the ink receptivity and print gloss development of model clay coating", Proceedings of 1994 International Printing and Graphic Arts Conference, TAPPI Press, Atlanta, 193-199.

36. MacPhee, J. (1997): "A Unified View of the Film Splitting Process, Part I", American Ink Maker, 75(1), p. 42 – 49.

37. Glatter, T. P., & Bousfield, D. W. (1996): "Print Gloss Development on Model Substrates", TAPPI International Printing and Graphic Arts Conference Proceedings, p. 139 – 147.

38. Preston, J. S., Parsons, D. J., Gate, L. F., Husband, J. C., Legrix, A., & Jones, M. (2002): "Ink Gloss Development Mechanisms at Short Time Scales After Printing – Part 1 – The Influence of Ink Film Thickness", 11th International Printing and Graphic Arts Conference Proceedings, Vol. 2, p. 1 – 10.

39. Donigian, D. W. (2006): "A Multiphase Mechanism for Setting and Gloss Development of Offset Ink", 2006 TAPPI Advanced Coating Fundamentals Symposium.

40. Ercan, S. N. (1998): "Influence of Process Parameters on Filament Size Distribution", 1998 Pan-Pacific and International Printing and Graphic Arts Conference Proceedings, p. 111 – 115.

41. Ercan, S. N. (2000): "Influence of Fluid Rheology on Filament Size", 2000 TAPPI International Printing and Graphic Arts Conference Proceedings, p. 121 – 132.

42. Voltaire, J., and Fogden, A. (2002): "Modeling Setting and Tack of a Sheet-fed Offset Ink Printed on a Coated Sheet", 11th International Printing and Graphic Arts Conference Proceedings.

43. Donigian, D. W., Vyorykka, J., Xiang, Y., and Bousfield, D. W. (2004): "The relationship between ink setting rates, backtrap piling and micro-picking", 2004 Coating and Graphic Arts Conference.

44. Pekarovicova, A. (2012): "Print Defects", WMU GPS 5100 Handouts.

45. Mottle (2005): Retrieved June 13, 2012, from http://www.spicers.com.au/index.asp?menuid=100.010&artid=346&function=NewsArticle

46. Anttila, M. and Hakkila, O. (2009): "Mottling in offset printing" 2009 TAPPI PaperCon conference presentation, St. Louis, MO.

47. Smith, D.A., Desjumaux, D., Kessler, H.H., Nicolas, N.R., Sharman, S. and Wright, A. (2004): "Operational principles and sensitivity of a new instrument designed to measure and explore offset ink tack dynamics, substrate failure and

ink transfer mechanisms " , Presentation slides in the Proceedings of International Printing and Graphic Arts Conference, Vancouver, Canada.

48. Gane, P. A. C. and Seyler, E. N. (1994): "Some novel aspects of ink/paper interaction in offset printing" Proceedings of International Printing and Graphic Arts Conference, p. 209-228.

49. Ink Surface Interaction Tester (ISIT) (2012), Retrieved June 13, 2012, from http://segan.co.uk/

50. Plowman N., "Ink Tack–part 3: Surface Measurement" Gr. Arts Mon. vol. 61, no. 6, Jun. (1989) p. 114.

51. Xiang, Y., Bousfield, D., Hassler, J., Coleman, P. and Osgood, A.(1999): "Measurement of local variation of ink tack dynamics", Journal of Pulp and Paper Science, Vol. 25, NO.9, Sep. p. 326-330.

52. Preston, J. S., Elton, N. J., Husband, J. C., Dalton, J.S., Heard, P.J., and Allen, G.C. (2002):"Investigation into the distribution of ink components on printed coated paper part 1: Optical and roughness considerations", Colloids and Surface A. 205, p. 183-115.

53. Beland, M. and Bennett, J. M. (2000):"Effect of local micro roughness on the gloss uniformity of printed paper surface", Applied Optics, 39(16), 2719-2726.

54. Chinga, G., Helle, T., and Johnsen, P. O., (2000):"Characterization of pigment coating layer structure using SEM and digital image analysis techniques", Proceedings of Coating & Graphic Arts Conference, Washington, DC.

55. Preston, J. S., Nutbeem, C, Parsons, J., and Jones, A., (2001):"The printability of coated papers with controlled microstructure", Paper Technology, 42(2), p. 33-41.

56. E.W. Washburn, Proc. Nat. Acad. Sci., 7, 115 (1921).

57. Paul A. Webb (2001): "An introduction to the physical characterization of materials by mercury intrusion porosimetry with emphasis on reduction and presentation of experimental data". Retrieved June 13, 2012, from www.particletesting.com/docs/intro_mip.pdf

58. Vidal D., and Bertrand F., (2006):"Recent progress and challenges in the numerical modeling of coating structure development", 2006 TAPPI Advanced Coating Fundamentals Symposium, Turku, Finland.

59. Pore-Cor homepage, Retrieved June 13, 2012, from http://www.pore-cor.com/about.htm

60. Pal, L., Joyce, M. and Fleming, P.D. (2006): "A simple method for calculation of the permeability coefficient of porous media", TAPPI Journal September, p. 10.

61. Darcy, H. (1856): "Les Fontaines Publiques de la Ville de Dijon", Dalmont, Paris.

62. Owens D. K. and Wendt R. C. (1969): "Estimation of the Surface Free Energy of Polymers", J. Appl. Pol. Sci., 13 (1969), p.1741.

63. Van Gilder, R.L., and Purfeerst, R.D. (1994): "Latex binder modification to reduce coating pick on six-color offset presses", TAPPI Journal, 77, 5, p. 230.

64. Van Gilder, R.L., and Smith, D. (1999): "Development of high polarity latex polymer for waterless sheet fed offset paper coatings", Proceedings of PITA coating conference, Edinburgh, UK, p. 50-56.

65. Kan, C.S. and Van Gilder, R.L. (2004): "Measurement of latex surface energy and its role in paper coating applications", Proceedings of 2004 TAPPI Coating and Graphic Arts Conference and Exhibit, p. 231-245.

APPENDIX

Table 14 Grade names of pigments

Label	**Grade Name**
CC	Hydrocarb 60
UF	Carbital 95

Table 15

The output from Minitab software about 3-variable 2-level study of ink tack build slope on all coated papers

Factorial Fit: Slope versus Base Paper, Pigment Type, Latex Level, Latex Type

Estimated Effects and Coefficients for Slope (coded units)

Term	Effect	Coef	SE Coef	T	P
Constant		0.656	0.1018	6.04	0.000
Base Paper	0.0538	0.0269	0.1018	0.26	0.797
Pigment Type	0.7238	0.3619	0.1018	3.55	0.005
Latex Level	0.6063	0.3031	0.1018	2.98	0.013
Latex Type	-0.5112	-0.2556	0.1018	-2.51	0.029

S = 0.407400 PRESS = 3.86268

R-Sq = 71.69% R-Sq(pred) = 40.10% R-Sq(adj) = 61.39%

Analysis of Variance for Slope (coded units)

Estimated Effects and Coefficients for Slope (coded units)

Source	DF	Seq SS	Adj SS	Adj MS	F	P
Main Effects	4	4.62248	4.62248	1.15562	6.96	0.005
Base Paper	1	0.01156	0.01156	0.01156	0.07	0.797
Pigment Type	1	2.09526	2.09526	2.09526	12.62	0.005
Latex Level	1	1.47016	1.47016	1.47016	8.86	0.013
Latex Type	1	1.04551	1.04551	1.04551	6.30	0.029
Residual Error	11	1.82572	1.82572	0.16597		
Total	15	6.44819				

Unusual Observations for Slope

Obs	StdOrder	Slope	Fit	SE Fit	Residual	St Resid
7	7	2.33000	1.56313	0.22774	0.76687	2.27R

R denotes an observation with a large standardized residual.

Table 16

The output from Minitab software about 3-variable 2-level study of coating failure forces on all coated papers

Factorial Fit: Failure Force versus Base Paper, Pigment Type, Latex Level, Latex Type

Estimated Effects and Coefficients for Failure Force (coded units)

Term	Effect	Coef	SE Coef	T	P
Constant		22.300	0.3287	67.85	0.000
Base Paper	0.325	0.162	0.3287	0.49	0.631
Pigment Type	3.775	1.888	0.3287	5.74	0.000
Latex Level	0.475	0.237	0.3287	0.72	0.485
Latex Type	-3.500	-1.750	0.3287	-5.32	0.000

S = 1.31469 PRESS = 40.2248

R-Sq = 84.95% R-Sq(pred) =68.16% R-Sq(adj) = 79.48%

Analysis of Variance for Failure Force (coded units)

Source	DF	Seq SS	Adj SS	Adj MS	F	P
Main Effects	4	107.328	107.328	26.8319	15.52	0.000
Base Paper	1	0.422	0.422	0.4225	0.24	0.631
Pigment Type	1	57.003	57.003	57.0025	32.98	0.000
Latex Level	1	0.903	0.902	0.9025	0.52	0.485
Latex Type	1	49.000	49.000	49.0000	28.35	0.000
Residual Error	4	19.012	19.012	1.7284		
Total	15	126.340				

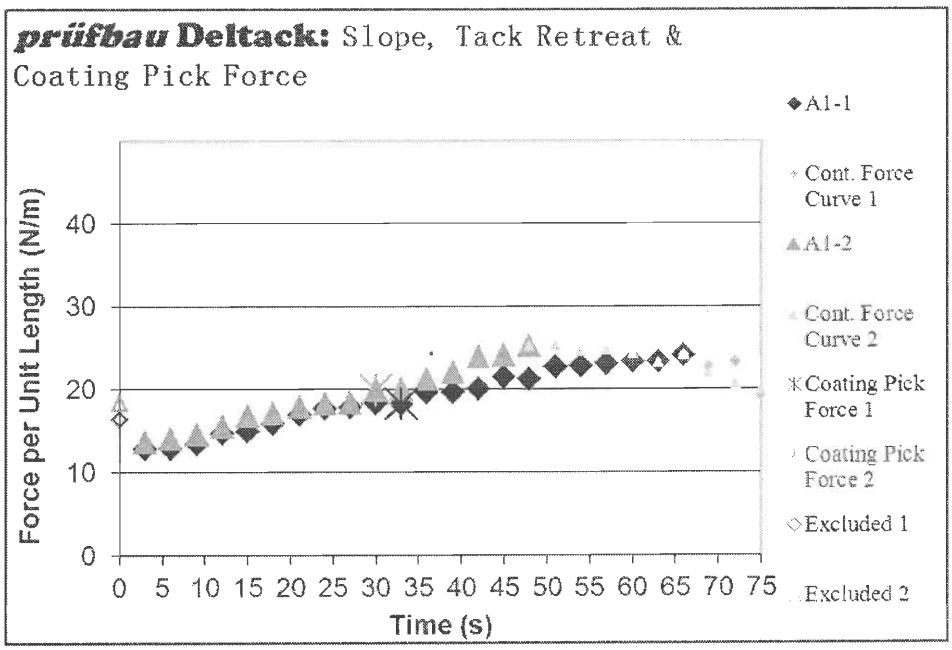

Figure 42: The ink setting force-time curve on the coated paper A1

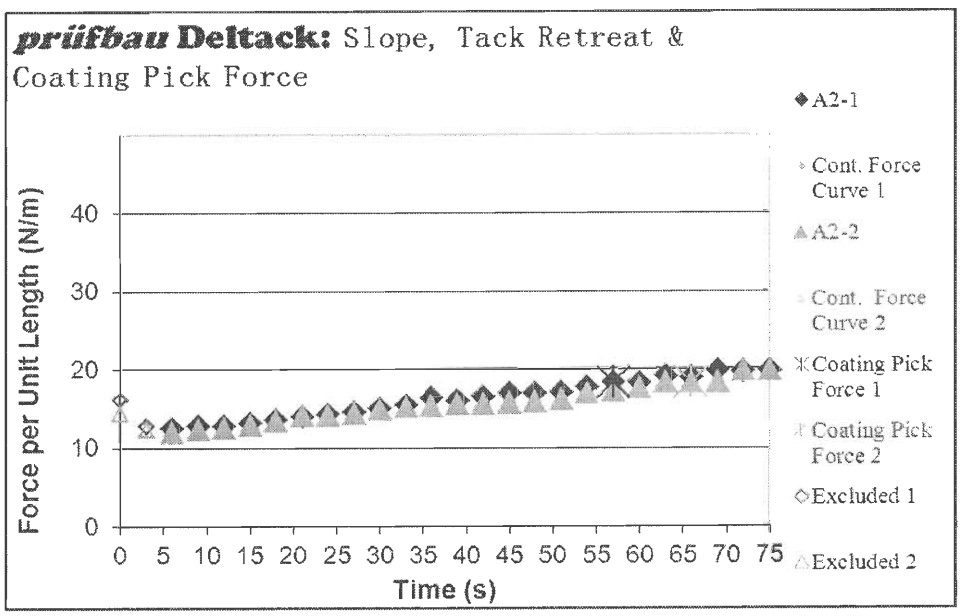

Figure 43: The ink setting force-time curve on the coated paper A2

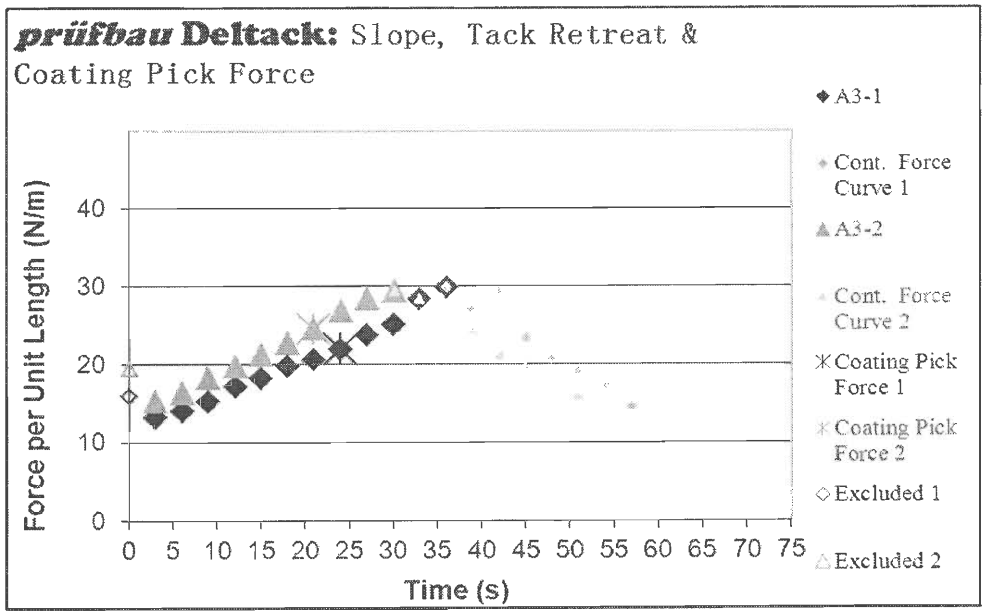

Figure 44: The ink setting force-time curve on the coated paper A3

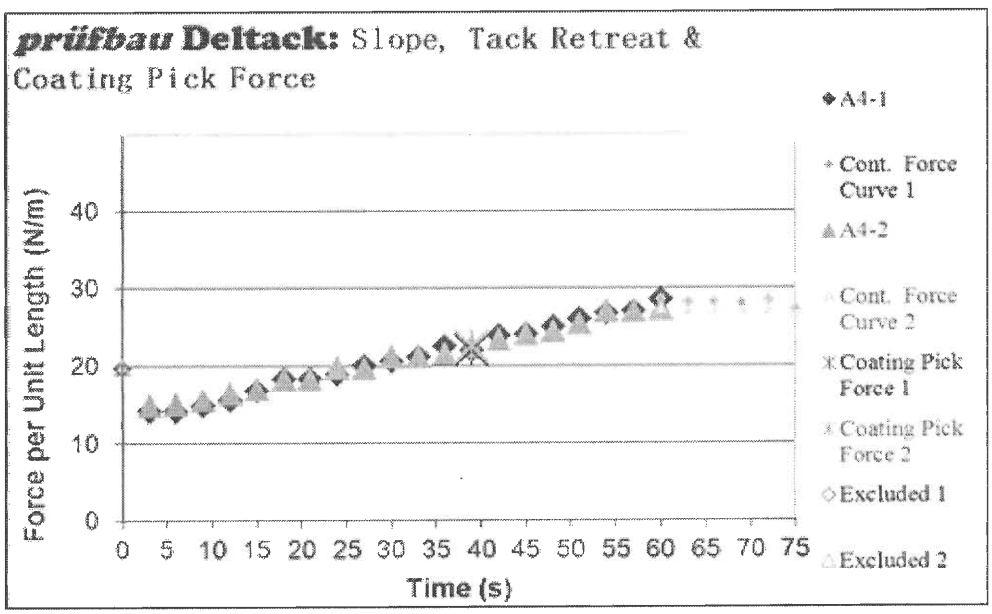

Figure 45: The ink setting force-time curve on the coated paper A4

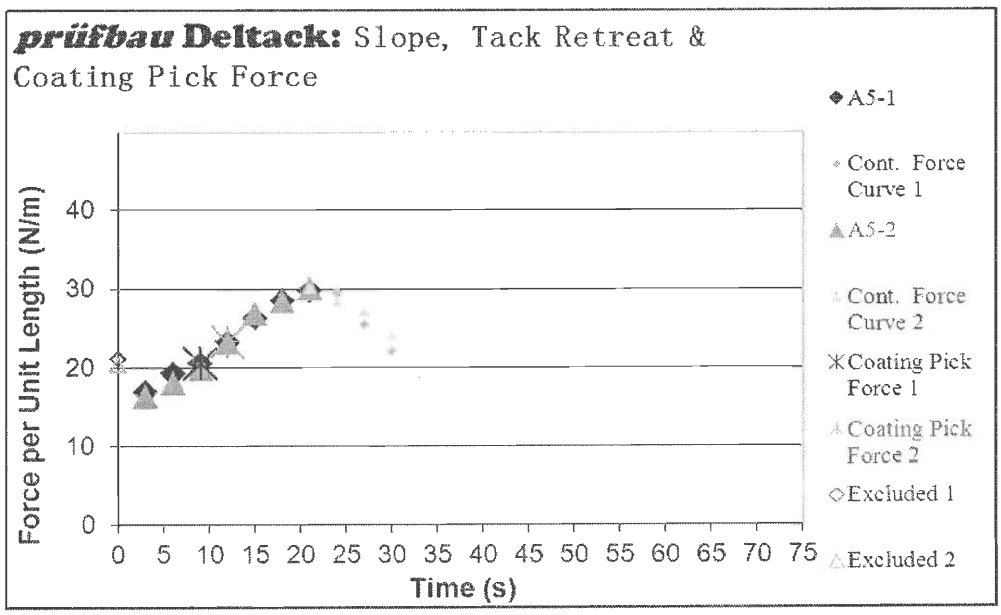

Figure 46: The ink setting force-time curve on the coated paper A5

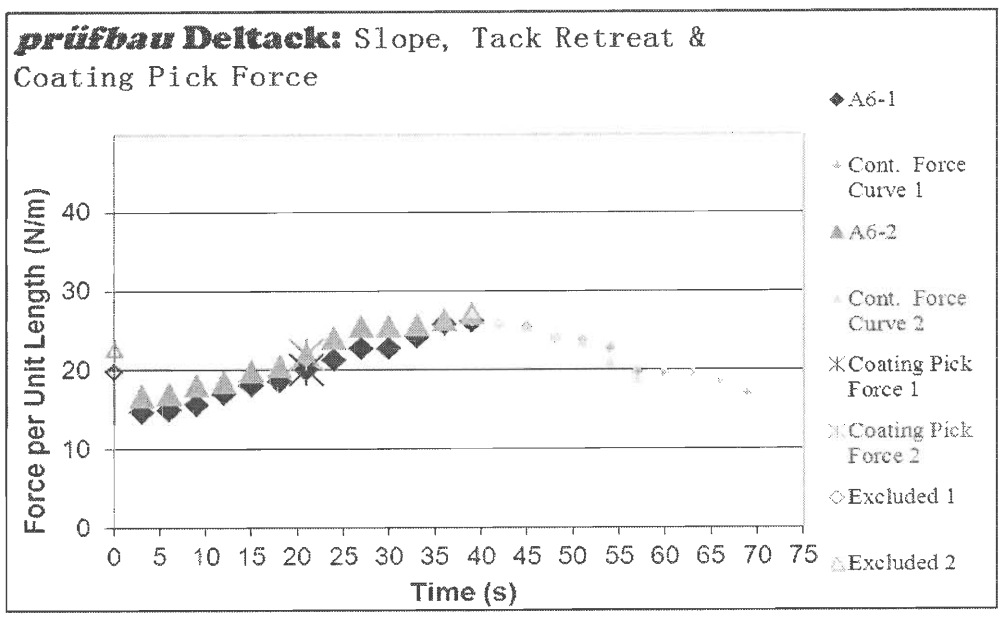

Figure 47: The ink setting force-time curve on the coated paper A6

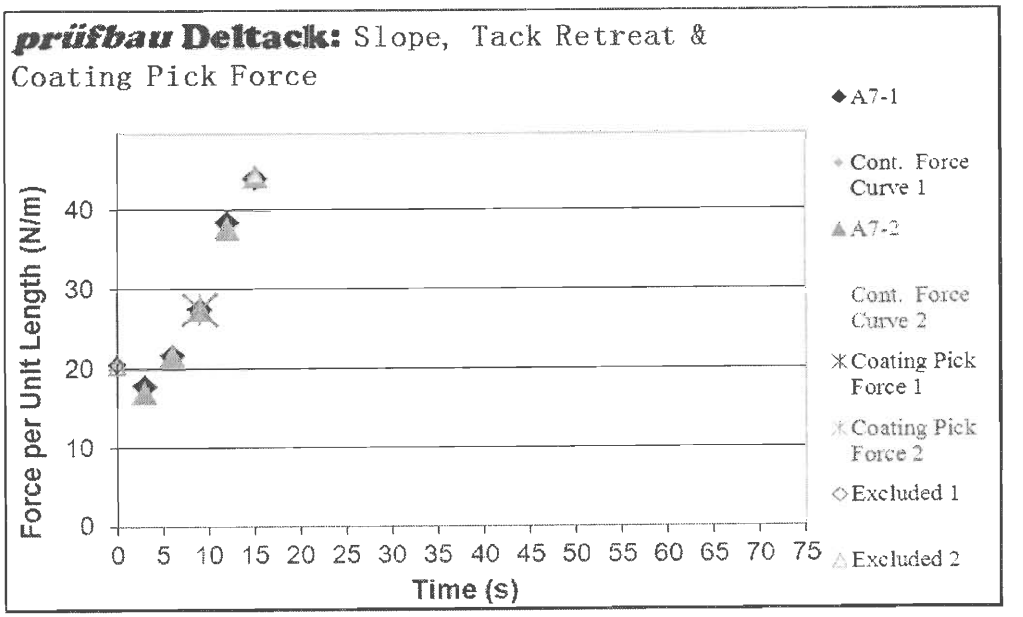

Figure 48: The ink setting force-time curve on the coated paper A7

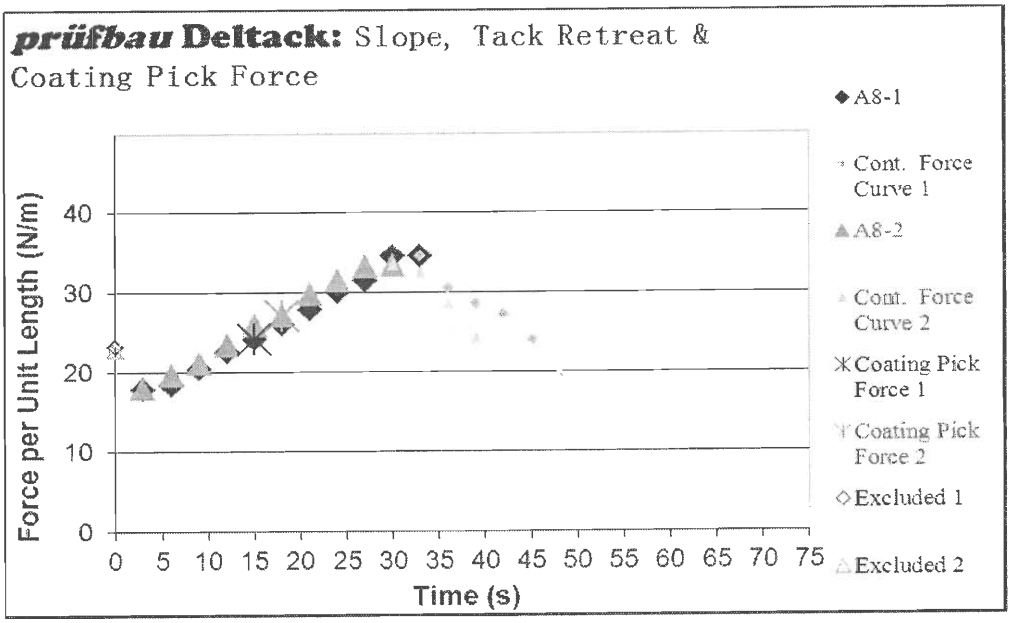

Figure 49: The ink setting force-time curve on the coated paper A8

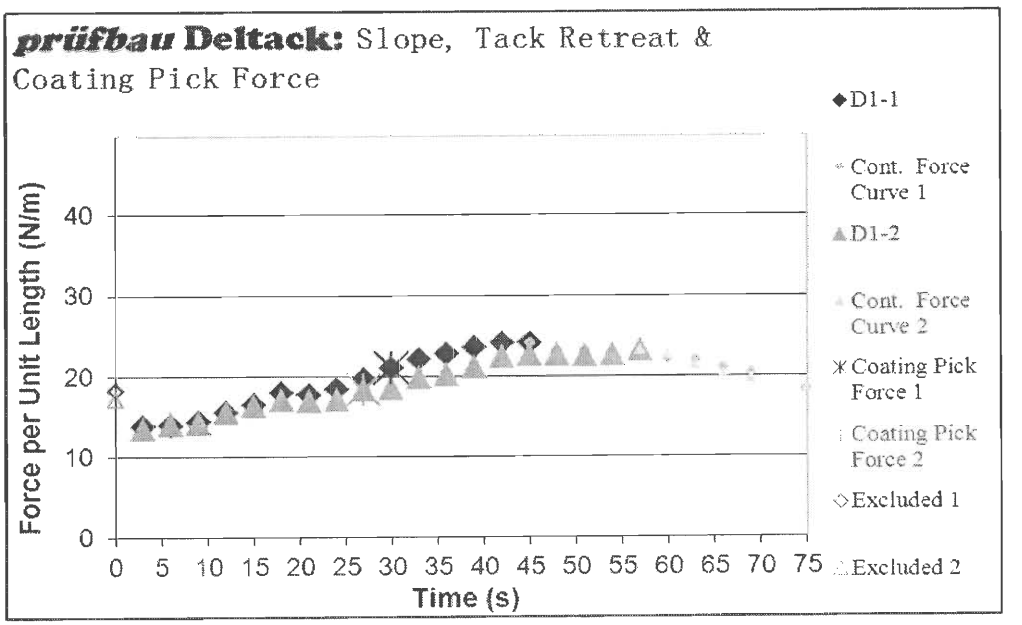

Figure 50: The ink setting force-time curve on the coated paper D1

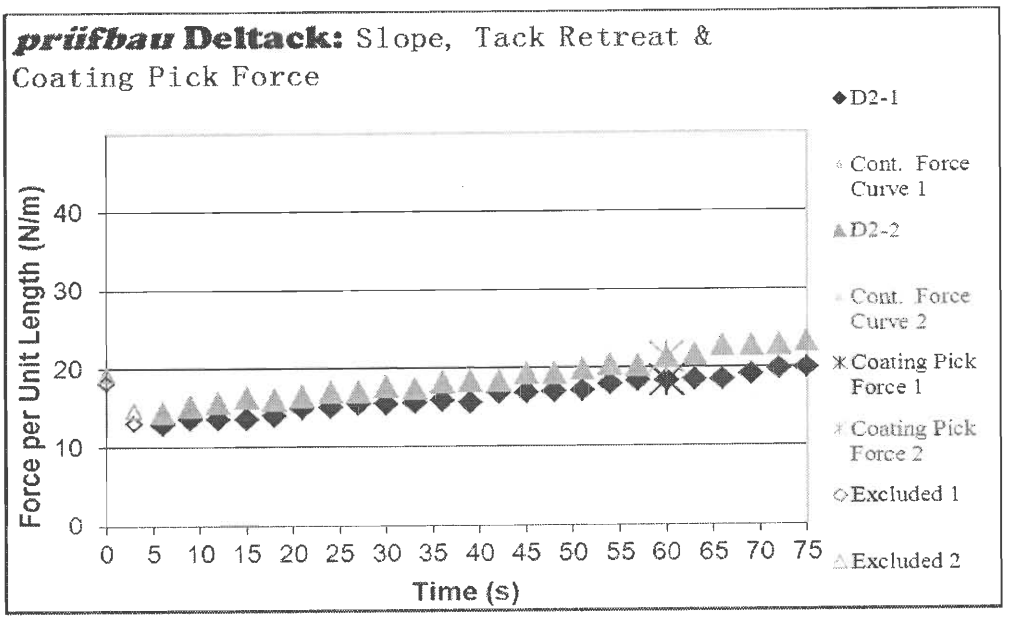

Figure 51: The ink setting force-time curve on the coated paper D2

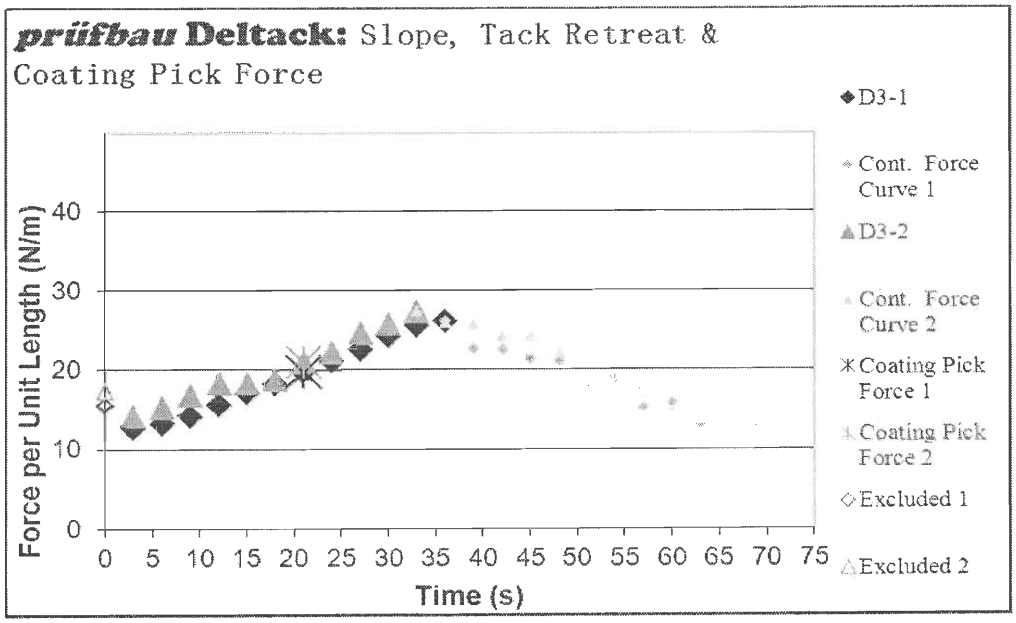

Figure 52: The ink setting force-time curve on the coated paper D3

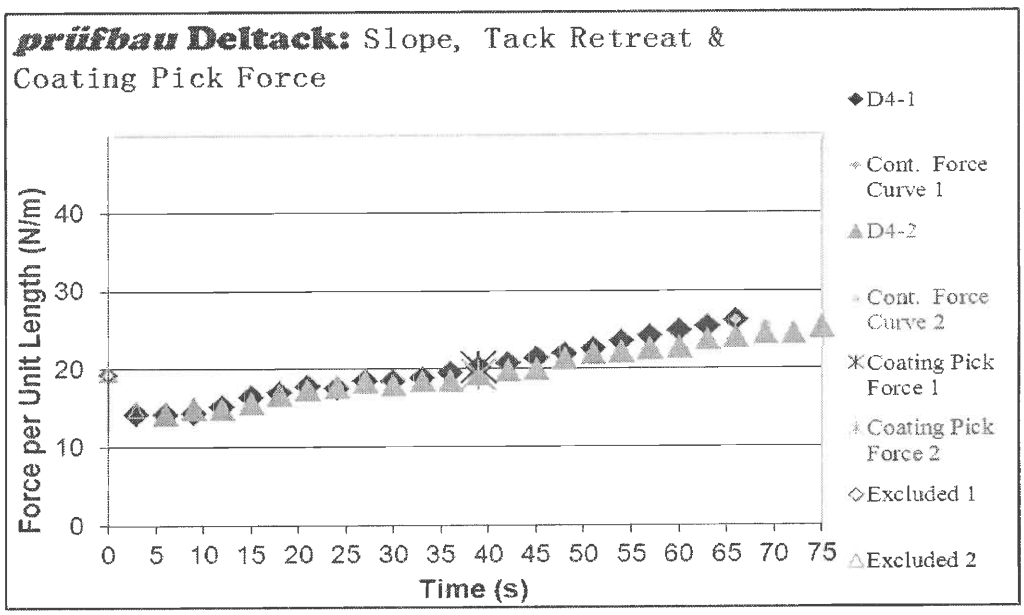

Figure 53: The ink setting force-time curve on the coated paper D4

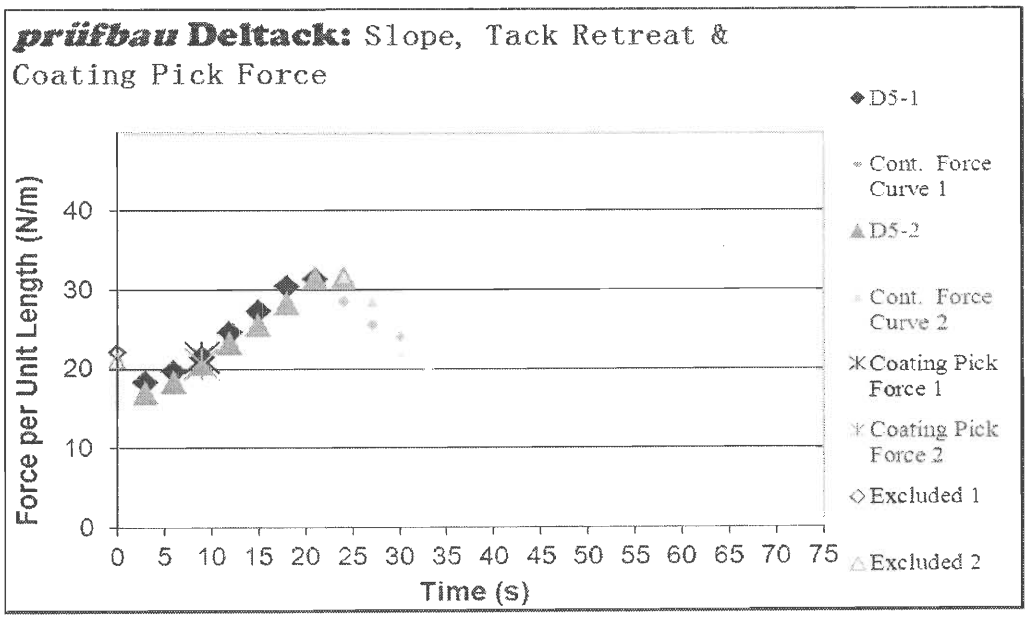

Figure 54: The ink setting force-time curve on the coated paper D5

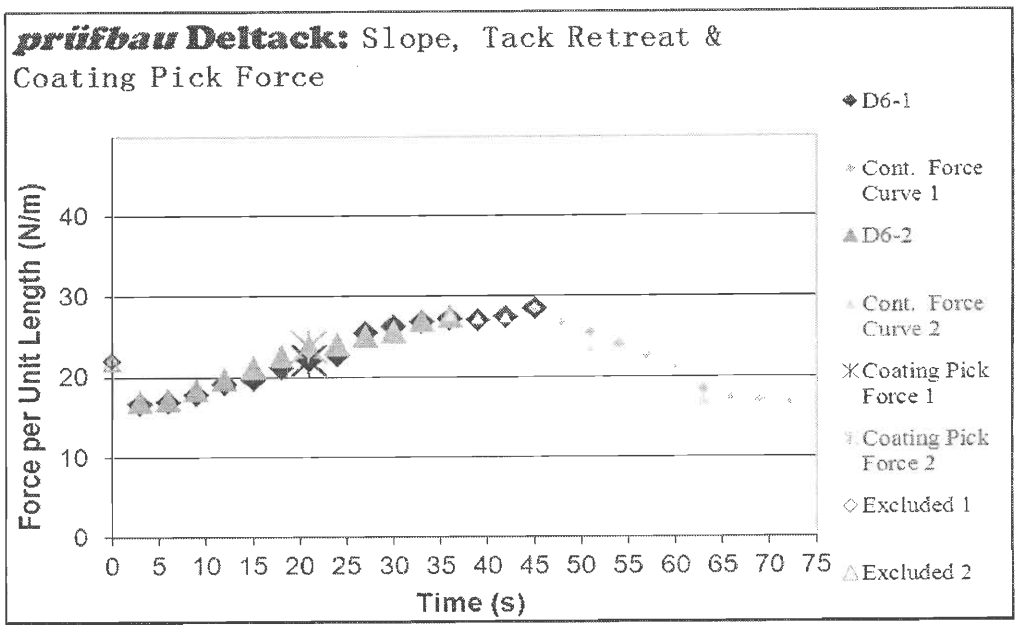

Figure 55: The ink setting force-time curve on the coated paper D6

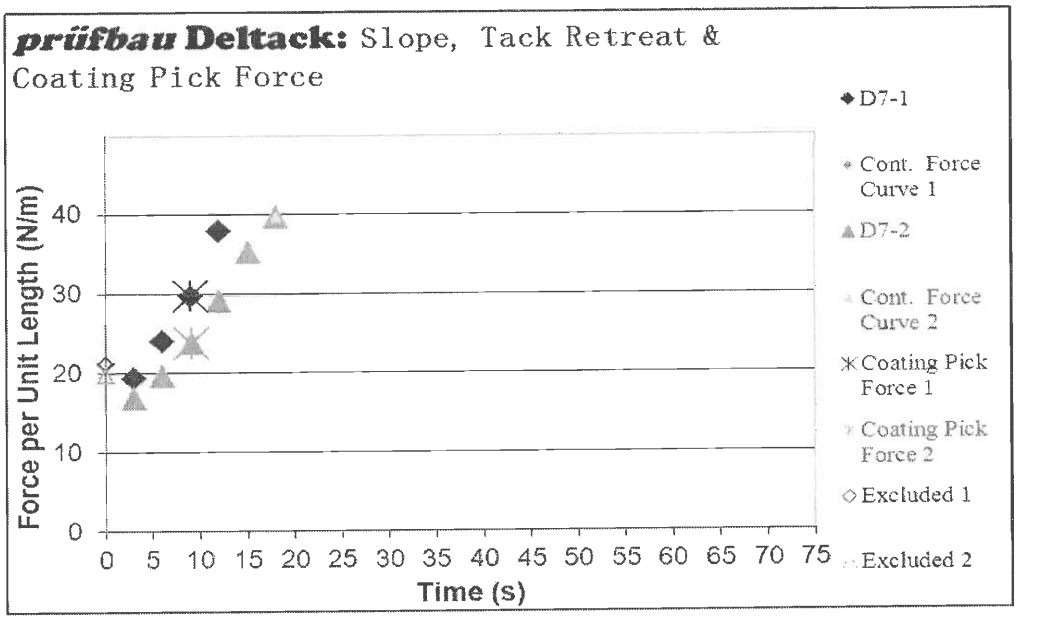

Figure 56: The ink setting force-time curve on the coated paper D7

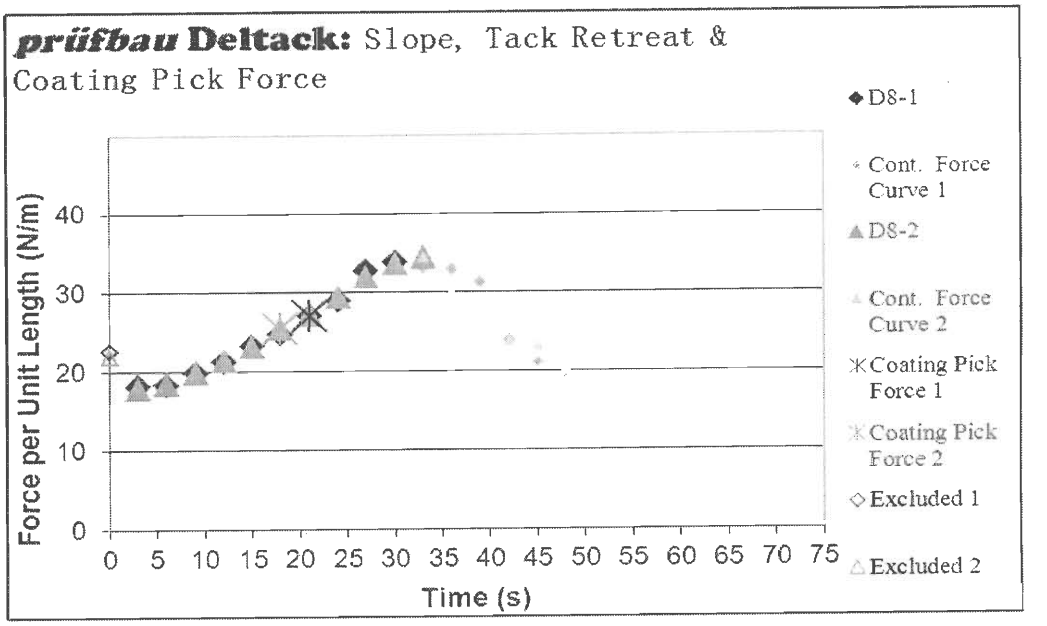

Figure 57: The ink setting force-time curve on the coated paper D8